CERTIFICATION OF APPROVAL

EFFECT OF WATER DEPTH ON THE BEHAVIOUR OF SPAR PLATFORM

by

Mohd Rasydan bin Bahrom

A project dissertation submitted to the
Civil Engineering Programme
Universiti Teknologi PETRONAS
in partial fulfilment of the requirement for the
Bachelor of Engineering (Hons)
(Civil Engineering)

Approved:

(Assoc Prof. Dr Kurian V. John)
Project Supervisor

Dr Kurian V. John
Associate Professor
Civil Engineering Department
Universiti Teknologi PETRONAS
Bandar Seri Iskandar, 31750 Tronoh
Perak Darul Ridzuan, MALAYSIA

UNIVERSITI TEKNOLOGI PETRONAS
TRONOH, PERAK

July 2008

CERTIFICATION OF ORIGINALITY

This is to certify that I am responsible for the work submitted in this project, that the original work is my own except as specified in the references and acknowledgements, and that the original work contained herein have not been undertaken or done by unspecified sources or persons.

(Mohd Rasydan bin Bahrom)

ABSTRACT

Deep water exploration has been one of major focus in oil and gas industries and companies. This paper discuss about the effect of water depth on the response of spar platform. It also discuss about effect of drag and mass coefficient for tubular member. The idea of this project is to find the motion and forces to the Spar platform with regards or influence of the water depth at certain locations. The case study is made with Genesis spar platforms in difference water depth. The equation that is used in finding the motions and forces is 'Linear Airy Wave Theory', 'Pierson-Moskowitz Spectrum' and 'Motion Response Spectrum'. The project also conducts a literature survey about the Spar Technology, Existing Spar, and Dynamic Analysis & Model Studies. The project will come up with tabulated result and some graphs about the effect of water depth on the spar responses. Some recommendation shall be include for further study and research.

ACKNOWLEDGEMENTS

After all the tough effort of studies and research, finally this final year project has been completed as planned without fail, Alhamdulillah. This work actually is combination various effort such as lecturer, friend and seniors. Therefore, the author takes this opportunity to express my appreciation for those who involve in this work

The author wishes to express his deep gratitude and appreciation to his project supervisor, Assoc. Prof. Dr Kurian V. John for his motivation, generous and patient supervision, comments, valuable suggestions and guidance throughout the study. Appreciation and thanks are also extended to his seniors, Ms Rosni and Ms Anis from the previous batch for their support and knowledge.

The author also would like to extend her appreciation to all her colleagues for their fully supports and collaboration. Last but not the least, the author wishes to express his heartfelt appreciation to her parents and family members for their moral support.

Hopefully, this work can be used and appreciated for those who are interested to make further studies or studies related to this field. The author felt very grateful to give contribution for the future development.

TABLE OF CONTENT

ABSTRACT III

ACKNOWLEDGEMENTS IV

CHAPTER 1 4

INTRODUCTION 4

1.1 BACKGROUND OF STUDY 4
1.2 PROBLEM STATEMENT 7
1.3 OBJECTIVES AND SCOPE OF STUDY 9
1.3.1 Objective 9
1.3.2 Scope of study 9

CHAPTER 2 10

LITERATURE REVIEW AND THEORY 10

2.1 EXPLORATION OF PETROLEUM 10
2.2 LINEAR AIRY WAVE THEORY 11
2.3 MORISON EQUATION 14
2.4 PIERSON-MOSKOWITZ SPECTRUM 15
2.5 WAVE PROFILE 16
2.6 MOTION-RESPONSE SPECTRUM 17

CHAPTER 3 18

METHODOLOGY 18

3.1 RESEARCH OF SPAR 18
3.2 PARAMETRIC STUDY OF THE RESPONSE WAVES TOWARDS SPAR WITH DIFFERENT PARAMETERS 18
3.3 RESEARCH FLOW CHART 19
3.3 HEALTH SAFETY AND ENVIRONMENT ISSUES 20

CHAPTER 4 21

RESULT AND CALCULATION 21

4.1 PLAN VIEW OF STRUCTURE AND FORCE IMPOSE 21
4.2 DIMENSION AND ENVIRONMENT DATA 22
4.3 ANALYSIS OF WAVE SPECTRUM 23
4.4 ANALYSIS ON WAVE PROFILE 25
4.5 ANALYSIS ON MOTION RESPONSE 26
4.6 ANALYSIS ON PARAMETRIC STUDIES 38
4.7 ANALYSIS ON DRAG AND MASS COEFFICIENT FOR TUBULAR MEMBER 42

CHAPTER 5 47

CONCLUSION AND RECOMMENDATION 47

5.0 CONCLUSION AND RECOMMENDATION 47

REFERENCE 48

APPENDICES 49

LIST OF FIGURES

Figure 1: Development of offshore platform from shallow water to deepwater operation ... 4
Figure 2: Type of motion of floating object ... 14
Figure 3: Genesis spar platform ... 18
Figure 4: Genesis spar Hull dimension ... 21
Figure 5: Genesis spar platform dimension ... 22

LIST OF TABLE

*Table 1: Genesis Spar platform details ... 8
Table 2: Dimension of Genesis spar platform: ... 22
Table 3: Environment data ... 23
Table 4: Pierson-Moskowitz spectrum ... 23
Table 5: Wave profile calculation with vary of time ... 25
Table 6: Surge parameter details ... 26
Table 7: RAO surge calculation ... 27
Table 8: S surge spectrum calculation ... 28
Table 9: Surge responses profile calculation ... 29
Table 10 : RAO parameter details ... 31
Table 11: RAO heave calculation ... 31
Table 12 : S heave spectrum calculation ... 32
Table 13: Heave responses profile calculation ... 33
Table 14: RAO pitch calculation ... 35
Table 15: S pitch spectrum calculation ... 36
Table 16: Pitch responses profile calculation ... 37
Table 17: Surge RAO^2 result for various water depths ... 39
Table 18: Heave RAO^2 result for various water depths ... 40
Table 19: Pitch RAO^2 result for various water depths ... 41
Table 20: Surge RAO^2 result for various combination of drag and mass coefficient ... 43
Table 21: Heave RAO^2 result for various combination of drag and mass coefficient ... 44
Table 22: Pitch RAO^2 result for various combination of drag and mass coefficient ... 46

LIST OF GRAPH

Graph 1: Pierson-Moskowitz spectrum for Genesis 24
Graph 2: Wave profile (wave height, m n(x,t) versus time, t) 26
Graph 3: RAO^2 surge versus frequency. 27
Graph 4: S surge spectrum 29
Graph 5: Surge displacement versus time, t 30
Graph 6: RAO^2 heave versus frequency. 32
Graph 7: S heave spectrum 33
Graph 8: Heave elevation versus time, t. 34
Graph 9: RAO pitch versus Frequency 35
Graph 10: S Pitch Spectrum 37
Graph 11: Pitch rotation versus time,t. 38
Graph 12: Surge RAO^2 for various water depths 41
Graph 13: Surge responses for various water depths 40
Graph 14: Heave RAO^2 for various water depths 42
Graph 15: Heave responses for various water depths 41
Graph 16: Pitch RAO^2 for various water depths 43
Graph 17: Pitch responses for various water depths 42
Graph 18: Surge RAO^2 for various Cd and Cm 44
Graph 19: Surge responses for various Cd and Cm 43
Graph 20: Heave RAO^2 for various Cd and Cm 46
Graph 21: Heave responses for various Cd and Cm 45
Graph 22: Pitch RAO^2 for various Cd and Cm 47
Graph 23: Pitch responses for various Cd and Cm 46

CHAPTER 1

INTRODUCTION

1.1 Background of study

Oil and gas has become primary power source in all over the world. Each country competes among each other to explore and extract more oil or gas. Nowadays, most of the sources lie deep beneath the sea bed. The exploration focus on the deeper water since the oil at the shallow water is depleting. A lot of innovation and research on offshore structure have been developing in order to improve the structure and reduce the cost of manufacture.

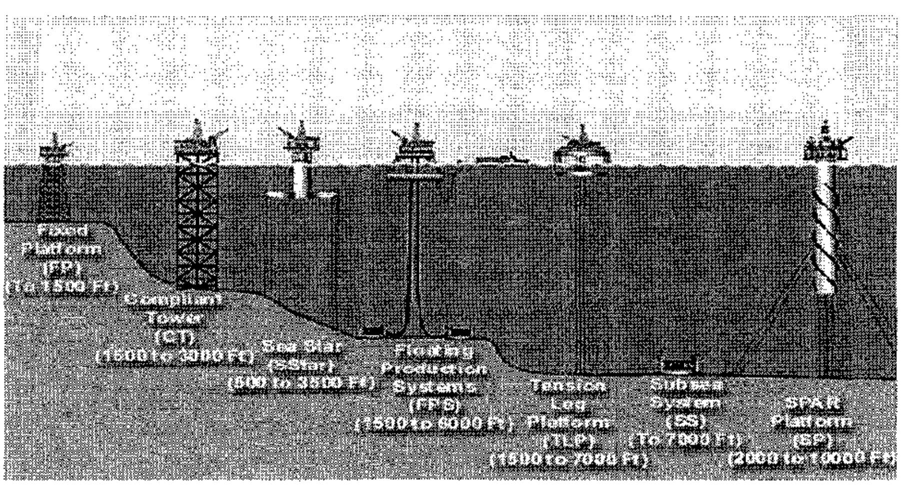

Figure 1: Development of offshore platform from shallow water to deepwater operation

Spar platform is one of floating structure which used in deepwater exploration for drilling, production, processing, storage, and offloading of ocean deposits. This is the next generation of deep water offshore structures which widely used by most of oil companies. The structure consists of a vertical cylinder, which floats vertically in the water. The bottom of the structure floats so deep in the water that the wave action at the surface is dampened by the counter balance effect of the structure weight. There are structures called strakes which look like a fins. The fins attached in a helical fashion around the exterior of the cylinder and act to break the water flow against the structure, further enhancing the stability.

Multi-component anchor lines are attached to the hull near its center of pitch for low dynamic loading and to keep the structure station. Because of the uncertainties related to the specification of the loads from the environment, it is major reason why analysis, design and operation for the spar platform become a tough job. Basically, current generations of Spar platforms are made of the following features: *(A.K Agarwal, A.K Jain "Dynamic Behavior of Offshore Spar platform under Regular Waves" Engineering 30 (2003) 487-516)*

(a) It can have a large range of topside payloads,
(b) The mooring system is easy to install, operate and relocate,
(c) It has favorable motions compared to other floating structures,
(d) It can have a steel or concrete hull,
(e) It is always stable because center of buoyancy (CB) is above the center of gravity (CG)
(f) It can be operated till 3000 Mts. depth of water from full drilling and production to production only,

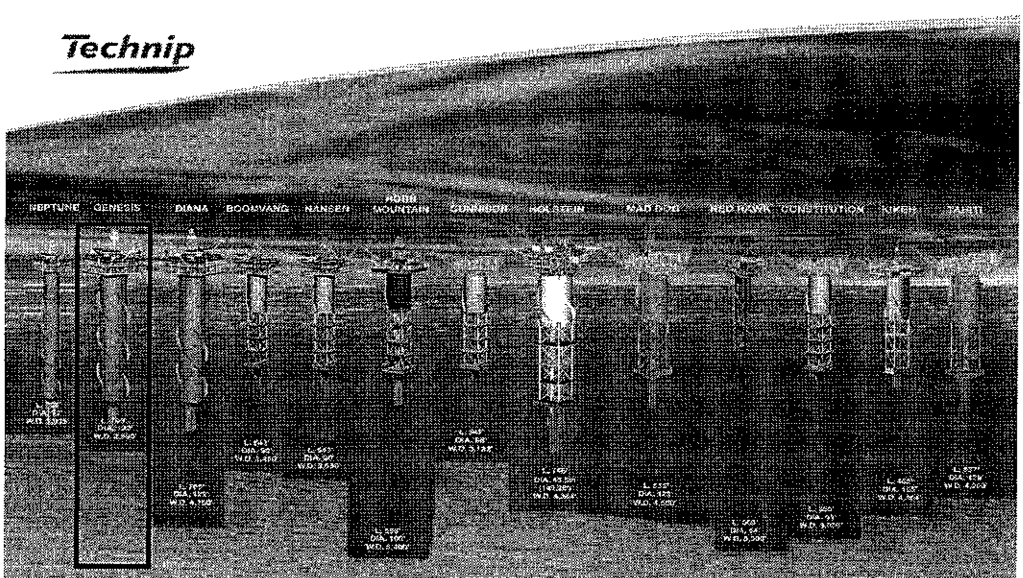

Figure 2: spar platforms installed with different water depth.

(g) Rigid steel production risers are supported in the center well by separate buoyancy cans,

(h) It has sea keeping characteristics superior to all other mobile drilling units,

(i) It has minimum hull /deck interface,

(j) Oil can be stored at low marginal cost,

(k) It can be used as a mobile drilling rig,

(l) The risers, which normally take breathing in the wave zone from high waves on semi-submersible, drilling units would be protected inside the Spar platform. Sea motion inside the Spar platform center well would be minimal.

Various analysis and model tests have been performed on spar platform which considered different aspects of platform motion and tether dynamics. It is assumed that all applied forces act at the body of the structure. The force impose to the structure vary with vary of water depth. To calculate the load or force, the properties of the wave must be considered. Wave is represented with spectrum which called 'wave spectrum' ing Pierson-Moskowitz spectrum. Water depth is one of parameters that required producing the spectrum.

Equation that express the motion in matrix form, Morison's equation:

$$M_y \ddot{u} + C\dot{u} + Ku = P\left(\dot{v}, \ddot{v}\right)$$

Where the object is solved for u;

M_v = diagonal matrix of virtual mass

C = matrix for structural and viscous damping

K = square linear structural stiffness matrix

$P\left(\dot{v}, \ddot{v}\right)$ = the load vector where (v dot) and (v double dot) are the water velocity and water acceleration.

$\ddot{u}$ = structural acceleration

$\dot{u}$ = velocity

U = displacement

1.2 Problem Statement

Deep water exploration is moving toward deeper water in order to extract more oils and gases. To accomplish that, it needs a lot of researches and developments especially on the structure integrity and stability. Many University and research company had come up with different idea and result. Each result is determined with conducting experiment and theoretical calculation.

The structure or specifically the body of the spar is the most important part where the structure will experience forces which come from the waves and other seastate aspects. Each parameter gives its own characteristic of dynamic forces. Without right calculation and assumption it will turn to the sinking of the structure. With that situation, major loss will be experience and the image of the company will be affected.

There are so many failure will be arising such as cracking due to fatigue and breaking of mooring line. It includes the flexibility of the structure which causes nonlinearity to the structure material. With that, the design must dynamically design. An analysis at every point must be considered as the distribution of load is differ from one point to another.

Genesis spar platform is one of classic spar installed at Gulf of Mexico, USA. This platform is owned by Chevron (operator), Exxon and Petrofina Delaware. The details are shown in table 1.2.1. Genesis spar platform is taken as a case study in this thesis. The original behavior such as force and motion at original water depth is calculated. Then, the platform will be taken to other water depth to see the different in its behavior and stability.

*Table 1: Genesis Spar platform details

Location Information	
• General Location	GOM GC 160, 161, 205A
• Water Depth	2,599' (792.1 m)
Hull Information	
• Type	Classic (1 Gen.)
• Slots	20
• Diameter	122' (37.2 m)
• Length	705' (214.9 m)
• Freeboard	55' (16.8 m)
• Draft	650' (198.1m)
Weight	
• Topside	12 500 MT
• Facility Payload	16 950 MT
• Hull Dry	28 700 MT

*Source from 2004 worldwide survey of spars by Jessica W. Speer, Tillie Nutter of Mustang Engineering and E. Kurt Albaugh, PE of BHP Billiton

1.3 Objectives and Scope of Study

1.3.1 Objective

1. To prepare a detailed report about the Spar Technology, Classic Spars, Existing Spars, Dynamic Analysis & Model Studies (Genesis spar platform).
2. To conduct a simple dynamic rigid body analysis in time domain for a typical spar for determining the spar motions.
3. To conduct a parametric study of the above responses changing water depth.
4. To determine the effect of drag and mass coefficient for tubular member.

1.3.2 Scope of study

1. Research and study about the function, history and concept of Spar Platform. This study includes journals, latest news and development on spar platform as well as websites and reference books.
2. Study on how to calculate force impose to the structure and effect of wave and other seastate condition. Several formulae are chosen for this analysis and calculation such as Morisson equation and linear airy wave theory.
3. Analysis on parametric study as main scope of studies. Changing water depth value for the same type of spar in the same seastate condition. Analysis the different and effect to the stability of the structure.

CHAPTER 2

LITERATURE REVIEW AND THEORY

2.1 Exploration of petroleum

"The UK Offshore gas industry dates back to 1963 when exploration of the southern North Sea commenced following the discovery of large onshore gas field at Groningen in Holland. The first onshore gas field, the West Sole situated off the Humber Estuary, was discovered in 1965 and this was quickly followed by Leman gas field approximately 50 miles off the coast of East Anglia".*(Angus Mather, "Offshore Engineering, an introduction" (1995) 27-28)*

Petroleum exploration was started onshore before it went to offshore starting in shallow water. As the sources depleting in onshore and shallow water, technology on exploration and production in deepwater was pushed to be develop from time to time. It is because petroleum had high demand in world market. As a result to the development of the offshore technology, many structure such as Tension Leg Platform, Spar Platform and Subsea structure had widely use across the region.

"For 10 years deepwater has been the global exploration mantra, for good reason. Scores of massive fields have been uncovered from primarily three main regions; the Gulf of Mexico, offshore Brazil and offshore Angola and Nigeria in West Africa.
However, as with any oil or gas province, maturity is a fact of life which begs the questions; how much deepwater potential remains, and where will the big new discoveries come from?"(Kathy Shirly, 2008). Until now, deepwater potential is argued, how much deep can we go. Without technology and method they can afford to retrieve new wells or

sources. It is a must for researcher and developer to come out with new technology from time to time.

The world's first production Spar was the Neptune Spar installed in 1996 by Oryx Energy Company and CNG. The Neptune Spar has a hull 705 ft (215m) long with a 32 x 32ft^2 (10 x 10 m^2) centrewell and a diameter of 72 ft (22m). The mooring system consists of six lines consisting of wire rope and chain.

There are 12 Spars installed and recognized in this world. The first three production Spar consisted of a long cylindrical outer shell with hard tanks near the top to provide buoyancy of the structure. Next, n middle section was void for free flooding while the lower part consists of soft tanks. The tank were only used to allow horizontal floatation of the spar during installation process, also for holding fixed ballast, if necessary Subsequent Spar replaces the middle section with a truss structure to reduce weight and cost, and to reduce current drag. To minimize heave motions, horizontal plates were included between the trusses to trap mass in the vertical direction.

This research will more focus on calculation of wave with effect of water depth. The wave calculated will be used to determine the force to the platform. The critical part is calculation of wave force. It determined how strong the structure should be fabricated. 'Morison Equation' is used which assumes the force to be composed of inertia with drag forces linearly combined. The components involve an inertia (or mass) coefficient and a drag coefficient which must be determined experimentally. This equation is applicable when drag force is significant.

2.2 Linear Airy Wave Theory

Airy theory also called sinusoidal wave theory which is the simplest and most useful in the small amplitude wave theory. The assumption that wave height is smaller than wave length is taken for this theory to allow free surface boundary condition to be linearized. The wave height is dropped which are beyond the first order. As a result, it allows the free surface condition is satisfied at the mean water level, rather than at the oscillating free surface.

Wave length is obtained from the formula:

$$L = L_o\left[\tanh\left(2\pi d/L\right)\right]$$

Lo = deepwater wave length, $gT^2/2\pi$

d = water depth.

g = gravity acceleration.

T = wave period

Wave elevation is obtained from the formula:

$$\eta = \frac{H}{2}\cos\Theta$$

H = wave height

$\Theta = kx - \omega t$

$k = 2\pi/L$

x = horizontal coordinate

$\omega = 2\pi/T$

$t = time$

Horizontal water particle velocity is given by:

$$u = \frac{\pi H}{T}\frac{\cosh ks}{\sinh kd}\cos\Theta$$

s = distance from the mud line

Vertical water-particle velocity is:

$$v = \frac{\pi H}{T} \frac{\sinh ks}{\sinh kd} \sin \Theta$$

Horizontal water-particle acceleration is:

$$\dot{u} = \frac{2\pi^2 H}{T^2} \frac{\cosh ks}{\sinh kd} \sin \Theta$$

Vertical water-particle acceleration is:

$$\dot{v} = -\frac{2\pi^2 H}{T^2} \frac{\sinh ks}{\sinh kd} \cos \Theta$$

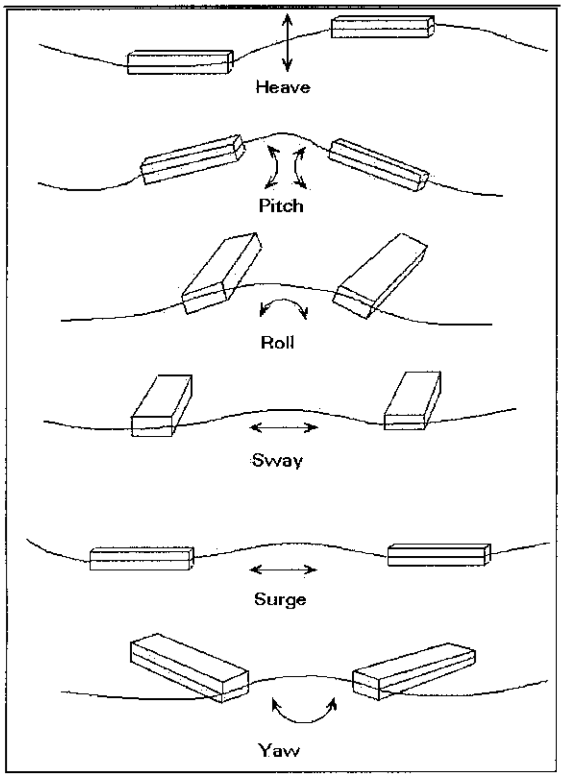

Figure 2: Type of motion of floating object

2.3 Morison Equation

This equation was developed by four guys in 1950 which were Morison, O'brien, Johnson and Shaaf. It is described the horizontal wave forces that acting on a vertical pile where the pile is extended from the bottom through the surface. There are two components forces which are exerted by the unbroken surface waves on a vertical pile which are inertia and drag force.

The concept of inertia force is where a water particle moving in a wave form carries along momentum with it. When the particle hit around the circular cylinder it accelerates and then decelerates. Inertia force equation:

$$Df_I = Cm\rho(\pi / 4)(D^2)\left(du/_{dt}\right)ds$$

Where,

Df_I = inertia force on the segment ds of the vertical cylinder.

D = cylinder diameter.

$du/_{dt}$ = local water particle acceleration at the centerline of the cylinder.

C_m = inertia coefficient.

ρ = water density

Drag force is proportional to the square of the water particle velocity. The situation occurs in a steady flow where downstream side is fixed. The case where oscillatory flow is occur, drag force has to be ensure in the same direction as the velocity by substituting the absolute value of the water particle. Drag force equation:

$$Df_D = \left(1/_2\right)C_d\rho D|U|uds$$

Where;

Df_D = drag force on an incremental segment, ds, of the cylinder

u = instantaneous water particle velocity

C_d = drag coefficient

The value of steady drag coefficient C_D is dependent on the Reynolds number and cylinder roughness in a steady flow. Experiment will define the smoothness and roughness of the cylinders. The cylinder roughness is directly proportional to the drag coefficient. In the case of the oscillatory flow this value is quite difficult to obtain.

The Morison equation (Drag + Inertia) is written as;

$$f = C_M A_1 \left(du/dt \right) + C_D A_D |u| u$$

Where;

f = force per unit length of the vertical cylinder

$A_1 = \rho \left(\pi/4 \right) \left(D^2 \right)$

$A_D = \left(1/2 \right) \rho D$

2.4 Pierson-Moskowitz spectrum

Pierson-Moskowitz spectrum was developed in 1964 by Pierson and Moskowitz which propose a new formula for an energy spectrum distribution of a wind generated sea state base on similarity theory of Kitaigorodskii and more accurate recorded data. This spectrum had widely been used by ocean engineer as representative for water all over the world.

The P-M spectrum model is formulated by:

$$S(f) = {ag^2}/{(2\pi)^4} f^{-5} \exp\left[-1.25\left(\frac{f}{f_o}\right)^{-4}\right]$$

a = 0.0081

g = gravitational acceleration

f = frequency

$$f_o = \frac{\sqrt{0.161g/H_s}}{2\pi}$$

Hs = significant wave height

2.5 Wave Profile

From the wave spectrum, the energy of the wave is translated to wave profile by calculating wave height by varies the time. Each time, t the height will be different and from the plotted graph, maximum height of random wave can be determined.

Horizontal coordinate is fixed, elevation of the wave for time, t is determined by:

$$\eta(x,t) = \sum {H(n)}/{2} \cos[k(n)x - 2\pi f(n)t + \varepsilon(n)]$$

$$H(f_I) = 2(2S(f_I)\Delta f)^{-4}$$

Where,

$\varepsilon(n) = Rn * 2\pi$

$\Delta f = 0.01$

2.6 Motion-Response Spectrum

Motion-response spectrum is theory used where a structure is move free in a wave and it may be critical near the resonance of the structure. The overall response of the platform is studied due to the design-wave spectrum. In this case, Pierson-Moskowitz spectrum is used. Total force is calculated for each frequency based on Pierson-Moskowitz spectrum. The formulas to get this motion response spectrum are:

$$S_{(f)Surge} = RAO^2{}_{surge} x S(f)$$

Where,

$S_{(f)surge}$ = motion response for surge force

$$RAO = \left[\frac{F_I / H/2}{\left[(K - m\omega^2)^2 + (C\omega)^2 \right]^{1/2}} \right] \eta_\beta(t)$$

S(f) = Pierson-Moskowitz spectrum

F_I = Total force

H = Wave height

K = Stiffness

C = Damping coefficient

η_β = Wave surface

CHAPTER 3

METHODOLOGY

3.1 Research of Spar

Genesis spar platform is selected as a case study. So far, a classic spar dimension has been collected. The dimension give a clear view how big is the platform and also how big is the force imposed. The dimension of Genesis spar is shown in figure 1.

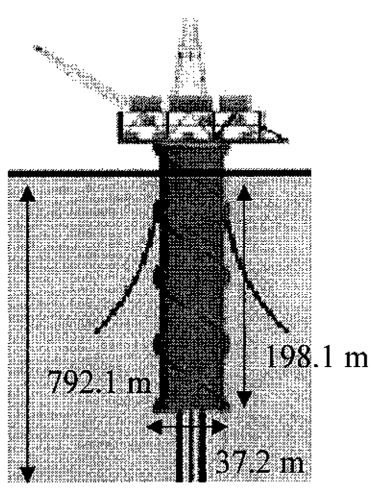

Figure 3: Genesis spar platform

3.2 Parametric study of the response waves towards Spar with different parameters

Linear Airy Wave theory and Pierson-Moskowitz Spectrum was used to define the characteristic of the wave profile. Until this stage, the research had capped until surge analysis of the structure. Then, the response theorem (RAO) is calculated base on the dimension and characteristic of the spar.

3.3 Research flow chart

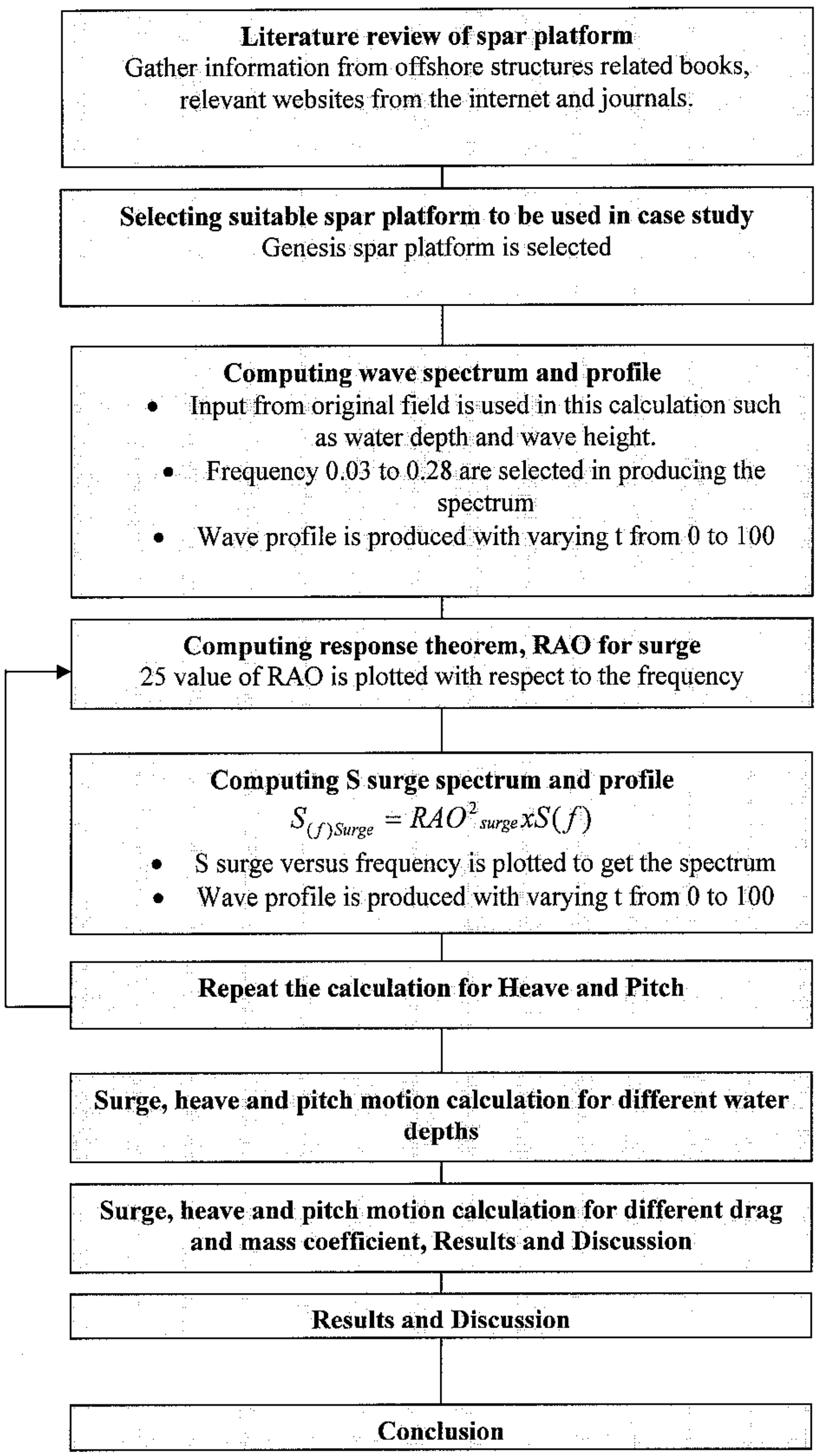

3.3 Health safety and environment issues

Offshore laboratory has been a place where all the testing of the model studies as well as to visualize wave and current reaction. It is important to have better understanding about those things. It will lead to the best researches done where it supported by experimental result and data.

In order to enter and conduct experiment and testing, HSE requirement must be follow. It is important to avoid any accident or unexpected tragedies. The rule and regulation that someone must follow are:

- Laboratory coat must be worn at all time in the lab
- Obey all instruction given by the technicians or lecturer.
- Full covered shoes must be worn at all time.
- Do not touch any equipment control without permission.
- Do report to the technician if there is unusual thing.

CHAPTER 4

RESULT AND CALCULATION

4.1 Plan view of structure and force impose

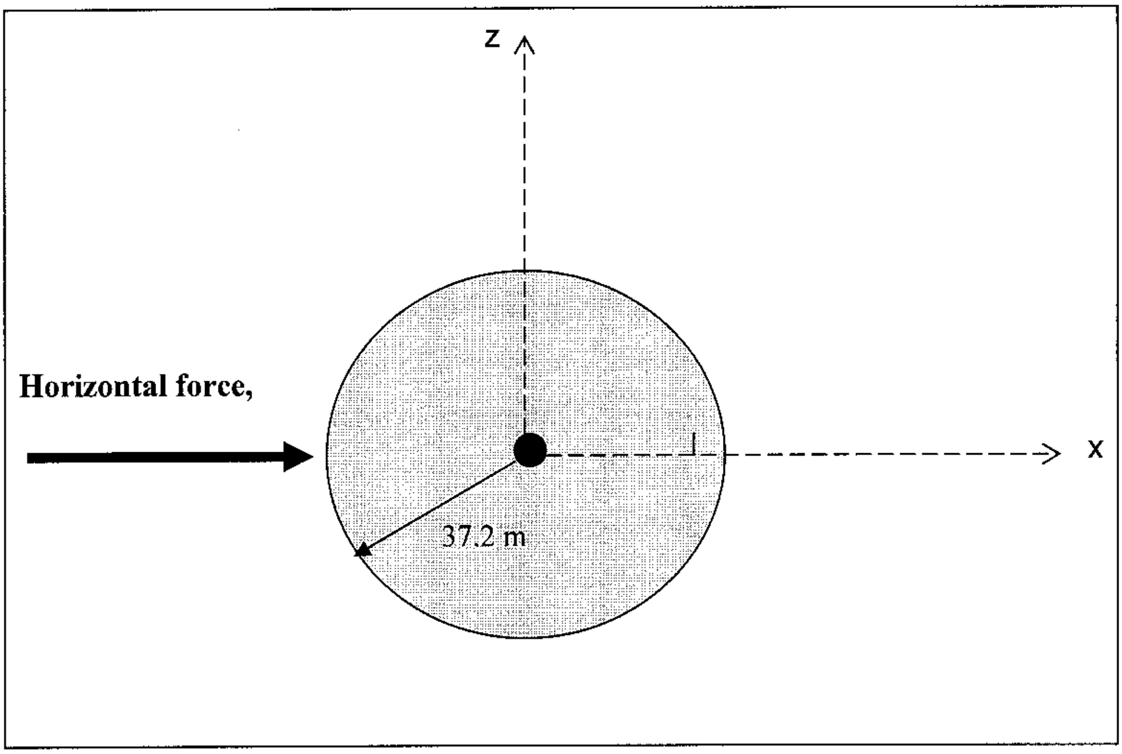

Figure 4: Genesis spar Hull dimension

Figure above explain the plan view of the structure with subject to the horizontal force. The force is imposed on a cylindrical shape or the hull of the platform. The force is calculated on each meter of water depth until the end of the hull. The total force is used in calculating response theorem, RAO. Z value is taken as 0 in this case.

4.2 Dimension and Environment data

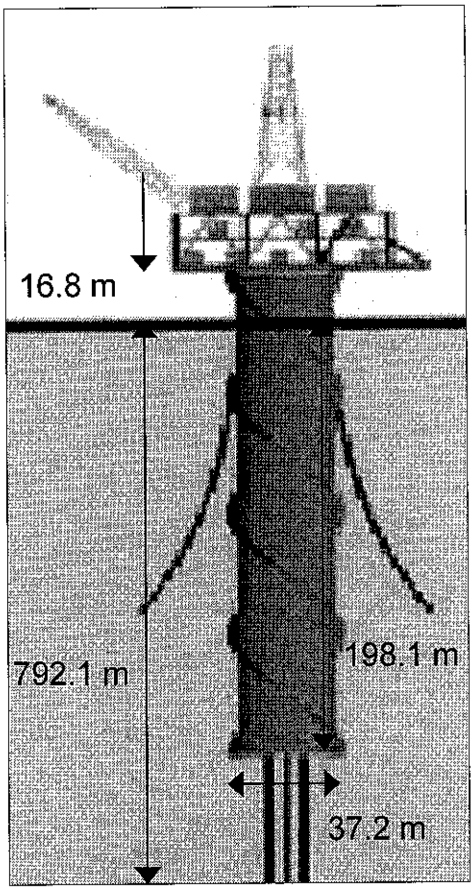

Figure 5: Genesis spar platform dimension

Table 2: Dimension of Genesis spar platform:

Hull Information	
• Type	Classic (1 Gen.)
• Slots	20
• Diameter	122' (37.2 m)
• Length	705' (214.9 m)
• Freeboard	55' (16.8 m)
• Draft	650' (198.1m)
Weight	
• Topside	12 500 MT
• Facility Payload	16 950 MT
• Hull Dry	28 700 MT

Table 3: Environment data

Significant wave height, m	10.7
Water depth, m	792.1

4.3 Analysis of wave spectrum

- **Pierson-Moskowitz spectrum**

$$S(f)=\frac{\alpha g^2}{(2\pi)^4} f^{-5} \exp\left[-1.25\left(\frac{f}{f_o}\right)^{-4}\right]$$

Table 4: Pierson-Moskowitz spectrum

f	*f* / *f*o	S(*f*)
0.035	0.572581388	0.084636067
0.045	0.73617607	38.38685069
0.055	0.899770753	147.384008
0.065	1.063365435	161.9469516
0.075	1.226960117	121.2497386
0.085	1.3905548	80.58194193
0.095	1.554149482	52.10202572
0.105	1.717744164	33.9019094
0.115	1.881338847	22.47507469
0.125	2.044933529	15.23807251
0.135	2.208528211	10.56907523
0.145	2.372122894	7.49098212
0.155	2.535717576	5.41670036
0.165	2.699312258	3.989136843
0.175	2.862906941	2.987121188
0.185	3.026501623	2.270884552
0.195	3.190096305	1.750286931
0.205	3.353690988	1.366039806
0.215	3.51728567	1.078412146
0.225	3.680880352	0.86030858
0.235	3.844475035	0.692946438
0.245	4.008069717	0.563105951
0.255	4.171664399	0.461350184
0.265	4.335259082	0.380853422
0.275	4.498853764	0.316617857

*f varies from 0.03 to 0.28

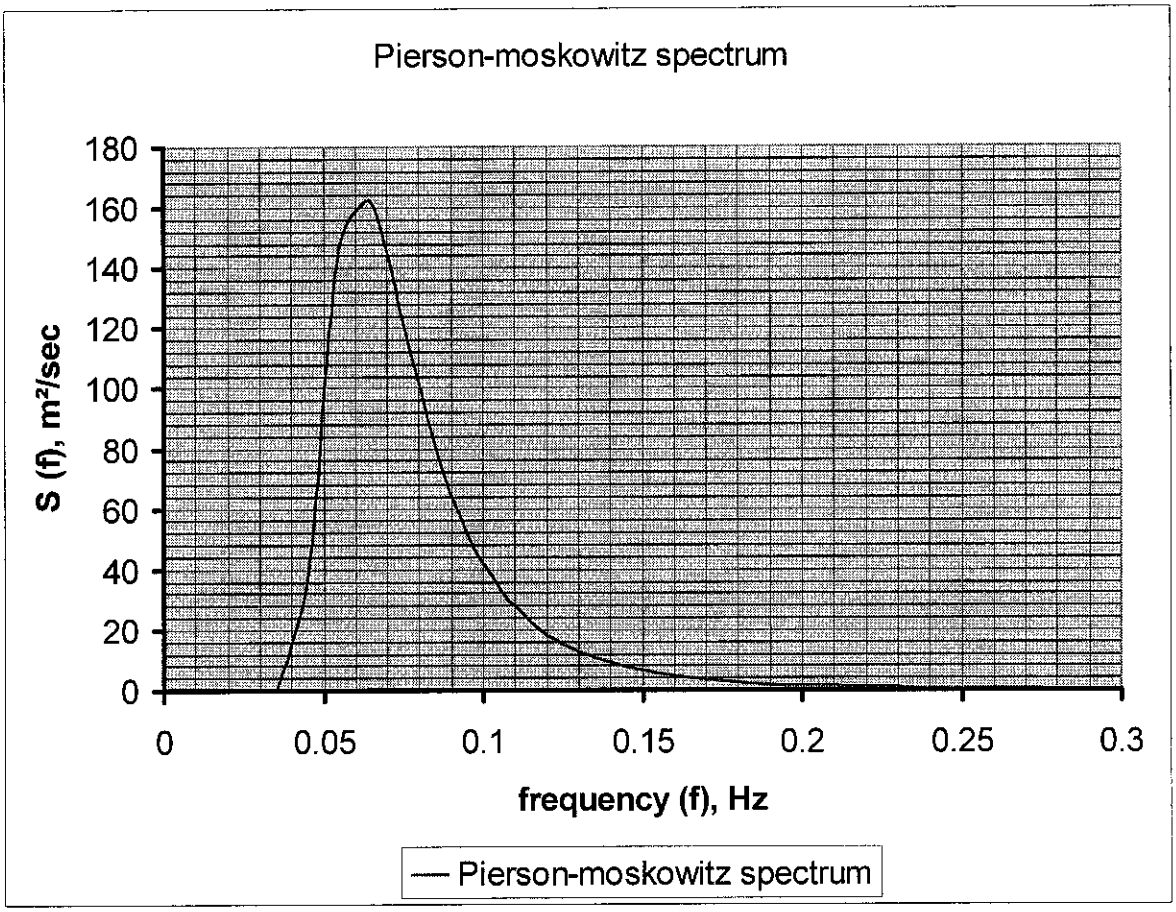

Graph 1: Pierson-Moskowitz spectrum for Genesis

S(f) or energy density for this wave profile show that the maximum value for this particular wave is 162 m^2. This value is affected by significant wave height which is 10.7 m. it affect through equation:

$$f_0 = \omega / 2\pi$$

$$f_0 = \frac{\sqrt{0.161g / H_s}}{2\pi}$$

$$f_0 = \frac{\sqrt{0.161(9.806) / 10.7}}{2\pi}$$

$$f_0 = 0.611$$

Fo is major parameter in caculating energy wave density where maximum energy is located.

4.4 Analysis on Wave Profile

$$\eta(x,t) = \sum_{n=1}^{N} \frac{H(n)}{2} \cos\left[k(n)x - 2\pi f(n)t + \varepsilon(n)\right]$$

$H(f_n) = 2\sqrt{2S(f_n)\Delta f}$ $\qquad\qquad\qquad\qquad$ $\varepsilon(n) = 2\pi Rn$

$$k(n) = \frac{2\pi}{L_n}$$

Table 5: Wave profile calculation with vary of time

t	f	f(n)	S(f)	H(f)	Rn	ε(n)	$\frac{H(n)}{2}\cos\left[k(n)x - 2\pi f(n)t + \varepsilon(n)\right]$
1	f1	0.035	0.084636	0.082285	0.201	1.263084	0.020715609
1	f2	0.045	38.38685	1.752412	0.634	3.984056	-0.742517383
1	f3	0.055	147.384	3.433762	0.597	3.751548	-1.657247426
1	f4	0.065	161.947	3.599411	0.744	4.675296	-0.775595474
1	f5	0.075	121.2497	3.114479	0.116	0.728944	1.505839633
1	f6	0.085	80.58194	2.539007	0.677	4.254268	-1.06291001
1	f7	0.095	52.10203	2.041608	0.577	3.625868	-1.014327419
1	f8	0.105	33.90191	1.646861	0.274	1.721816	0.401117725
1	f9	0.115	22.47507	1.340897	0.304	1.910336	0.250624726
1	f10	0.125	15.23807	1.104104	0.993	6.240012	0.373106673
1	f11	0.135	10.56908	0.919525	0.85	5.3414	-0.100032688
1	f12	0.145	7.490982	0.774131	0.572	3.594448	-0.347118339
1	f13	0.155	5.4167	0.658283	0.161	1.011724	0.328907393
1	f14	0.165	3.989137	0.564917	0.717	4.505628	-0.267475059
1	f15	0.175	2.987121	0.488845	0.495	3.11058	-0.104127749
1	f16	0.185	2.270885	0.426229	0.397	2.494748	0.050365546
1	f17	0.195	1.750287	0.374196	0.146	0.917464	0.178298461
1	f18	0.205	1.36604	0.33058	0.38	2.38792	0.075019108
1	f19	0.215	1.078412	0.293723	0.75	4.713	-0.143310432
1	f20	0.225	0.860309	0.262345	0.263	1.652692	0.127450206
1	f21	0.235	0.692946	0.235448	0.05	0.3142	0.046737535
1	f22	0.245	0.563106	0.212246	0.169	1.061996	0.094248801
1	f23	0.255	0.46135	0.192115	0.906	5.693304	-0.05593026
1	f24	0.265	0.380853	0.174552	0.858	5.391672	-0.07277161
1	f25	0.275	0.316618	0.159152	0.748	4.700432	-0.078438933
						n(x,t)	-2.969371366

varied from 1 to 100

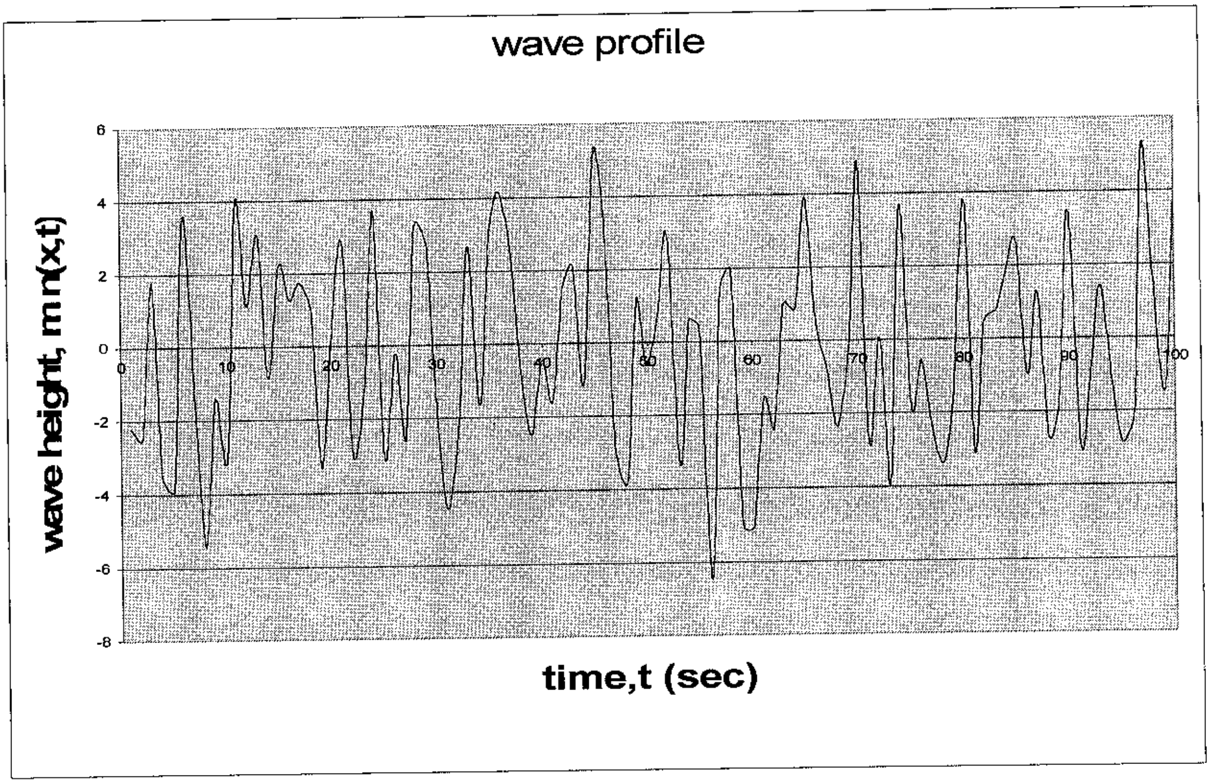

Graph 2: Wave profile (wave height, m n(x,t) versus time, t)

From the wave spectrum, wave profile has been developed using shown equation. The profile shows non linear fluctuation to the wave height due to random wave. The maximum wave height recorded in this profile is -6m which in 75 seconds.

4.5 Analysis on Motion response

- **RAO for Surge**

$$RAO = \left[\frac{F_I/(H/2)}{\left[(K - m\omega^2)^2 + (C\omega^2)\right]^{1/2}} \right]$$

Table 6: Surge parameter details

T spar	325	sec
Hs	10.7	m
K, stiffness	165734.5902	N/m
m	221655000	kg
Mtotal	443310000	kg
ς	0.1	
C	1714313.871	

Table 7: RAO surge calculation

Total force (N)	Frequency	S(*f*)	H	RAO	RAO²
96.07936617	0.035	0.084636067	0.08228539	0.012542156	0.000157306
48866.68288	0.045	38.38685069	1.752412068	0.210340614	0.044243174
194734.045	0.055	147.384008	3.433761879	0.590797044	0.349041147
216528.5474	0.065	161.9469516	3.599410525	0.354667005	0.125788684
163160.5921	0.075	121.2497386	3.114478943	0.168824079	0.02850157
109113.1356	0.085	80.58194193	2.539006765	0.089141027	0.007946123
71045.26089	0.095	52.10202572	2.041607714	0.051267106	0.002628316
46592.98905	0.105	33.9019094	1.646861485	0.031479068	0.000990932
31158.02703	0.115	22.47507469	1.340897451	0.020356553	0.000414389
21326.09136	0.125	15.23807251	1.104104071	0.013730817	0.000188535
14943.80484	0.135	10.56907523	0.919524887	0.009591913	9.20048E-05
10708.55191	0.145	7.49098212	0.774130848	0.006901982	4.76374E-05
7834.565425	0.155	5.41670036	0.658282636	0.005094036	2.59492E-05
5842.021362	0.165	3.989136843	0.564916762	0.003843303	1.4771E-05
4432.539757	0.175	2.987121188	0.488845267	0.002956083	8.73843E-06
3416.781185	0.185	2.270884552	0.426228535	0.002312732	5.34873E-06
2672.116361	0.195	1.750286931	0.374196412	0.001837056	3.37477E-06
2117.531444	0.205	1.366039806	0.330580073	0.001479208	2.18806E-06
1698.488093	0.215	1.078412146	0.29372261	0.001205786	1.45392E-06
1377.6161	0.225	0.86030858	0.262344595	0.000993921	9.8788E-07
1128.882525	0.235	0.692946438	0.235447903	0.000827655	6.85012E-07
933.8710107	0.245	0.563105951	0.212246263	0.000695651	4.83931E-07
779.3654355	0.255	0.461350184	0.192114588	0.000589733	3.47785E-07
655.7542381	0.265	0.380853422	0.174551636	0.000503912	2.53927E-07
555.959955	0.275	0.316617857	0.159152218	0.000433747	1.88136E-07

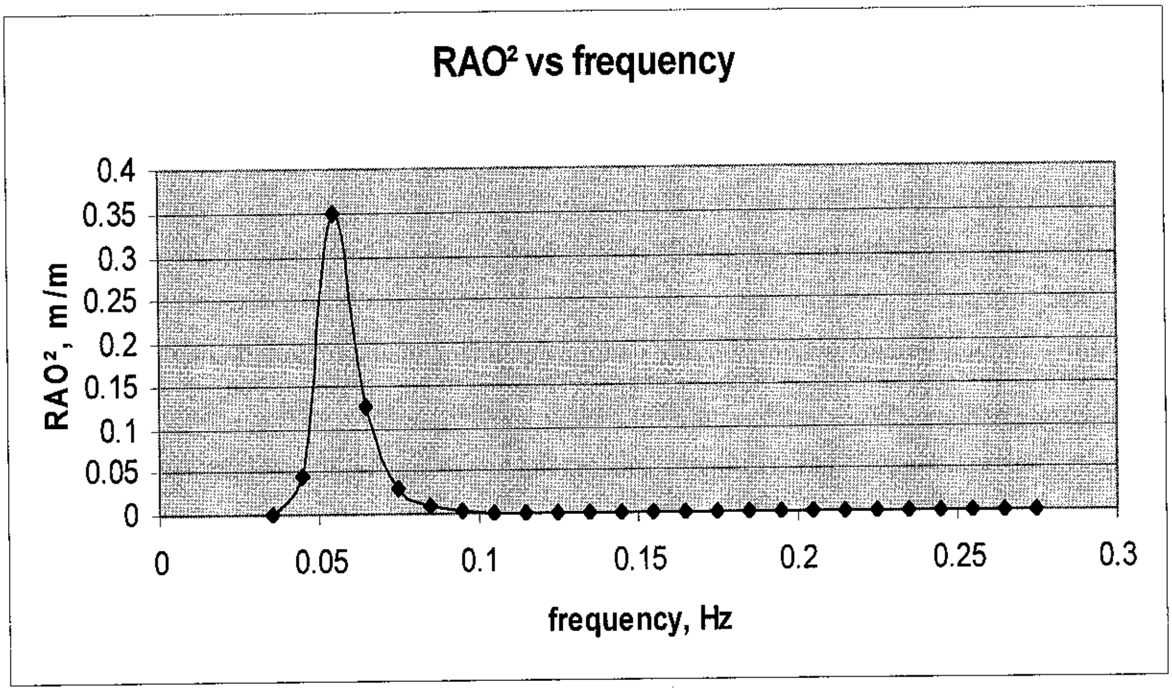

Graph 3: RAO² surge versus frequency.

- **S surge response spectrum**

$$S_{(f)Surge} = RAO^2_{surge} * S(f)_{wave}$$

Table 8: S surge spectrum calculation

frequency	S(f)	RAO²	S surge
0.035	0.084636067	0.000157306	1.33137E-05
0.045	38.38685069	0.044243174	1.698356105
0.055	147.384008	0.349041147	51.44308323
0.065	161.9469516	0.125788684	20.37109395
0.075	121.2497386	0.02850157	3.455807884
0.085	80.58194193	0.007946123	0.640313994
0.095	52.10202572	0.002628316	0.136940594
0.105	33.9019094	0.000990932	0.033594477
0.115	22.47507469	0.000414389	0.009313429
0.125	15.23807251	0.000188535	0.002872915
0.135	10.56907523	9.20048E-05	0.000972406
0.145	7.49098212	4.76374E-05	0.000356851
0.155	5.41670036	2.59492E-05	0.000140559
0.165	3.989136843	1.4771E-05	5.89235E-05
0.175	2.987121188	8.73843E-06	2.61027E-05
0.185	2.270884552	5.34873E-06	1.21463E-05
0.195	1.750286931	3.37477E-06	5.90682E-06
0.205	1.366039806	2.18806E-06	2.98897E-06
0.215	1.078412146	1.45392E-06	1.56792E-06
0.225	0.86030858	9.8788E-07	8.49881E-07
0.235	0.692946438	6.85012E-07	4.74677E-07
0.245	0.563105951	4.83931E-07	2.72504E-07
0.255	0.461350184	3.47785E-07	1.60451E-07
0.265	0.380853422	2.53927E-07	9.67091E-08
0.275	0.316617857	1.88136E-07	5.95674E-08

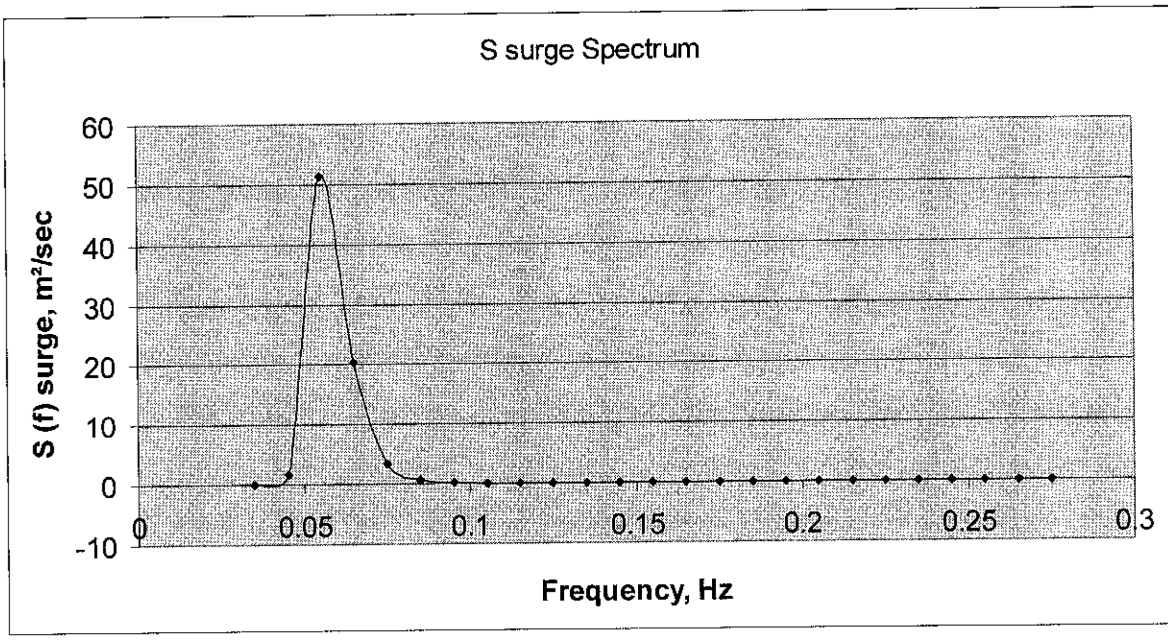

Graph 4: S surge spectrum

- **Surge Responses Profile**

Table 9: Surge responses profile calculation

t	*f*	f(n)	S(*f*)	H(*f*)	Rn	ε(n)	$\frac{H(n)}{2}\cos\left[k(n)x - 2\pi f(n)t + \varepsilon(n)\right]$
1	*f*1	0.035	1.33E-05	0.001032	0.155086	0.974558	0.000375936
1	*f*2	0.045	1.698356	0.368603	0.766127	4.814344	-0.033145109
1	*f*3	0.055	51.44308	2.028656	0.22363	1.405294	0.496165173
1	*f*4	0.065	20.37109	1.276592	0.02465	0.154903	0.617887421
1	*f*5	0.075	3.455808	0.525799	0.362291	2.276634	-0.061096224
1	*f*6	0.085	0.640314	0.22633	0.713194	4.481712	-0.078355875
1	*f*7	0.095	0.136941	0.104667	0.741579	4.660083	-0.03164186
1	*f*8	0.105	0.033594	0.051842	0.715731	4.497656	-0.019887942
1	*f*9	0.115	0.009313	0.027296	0.575239	3.614802	-0.013225593
1	*f*10	0.125	0.002873	0.01516	0.790429	4.967058	-0.003837439
1	*f*11	0.135	0.000972	0.00882	0.893253	5.613201	0.000231294
1	*f*12	0.145	0.000357	0.005343	0.154667	0.971929	0.002666591
1	*f*13	0.155	0.000141	0.003353	0.51829	3.256935	-0.001095594
1	*f*14	0.165	5.89E-05	0.002171	0.156665	0.984486	0.001084085
1	*f*15	0.175	2.61E-05	0.001445	0.597152	3.752502	-0.000637926
1	*f*16	0.185	1.21E-05	0.000986	0.686397	4.31332	-0.000492855
1	*f*17	0.195	5.91E-06	0.000687	0.083115	0.522297	0.0002622
1	*f*18	0.205	2.99E-06	0.000489	0.858101	5.392305	-0.000139725
1	*f*19	0.215	1.57E-06	0.000354	0.219093	1.376781	0.000177025
1	*f*20	0.225	8.5E-07	0.000261	0.690894	4.341578	-0.000127403
1	*f*21	0.235	4.75E-07	0.000195	0.050549	0.317652	3.8991E-05
1	*f*22	0.245	2.73E-07	0.000148	0.568912	3.575041	-3.30826E-05
1	*f*23	0.255	1.6E-07	0.000113	0.913446	5.740097	-3.07935E-05
1	*f*24	0.265	9.67E-08	8.8E-05	0.956691	6.011845	-1.57314E-05
1	*f*25	0.275	5.96E-08	6.9E-05	0.767646	4.823887	-3.44797E-05
						n(x,t)	0.875091083

***t is varied from 1 to 100**

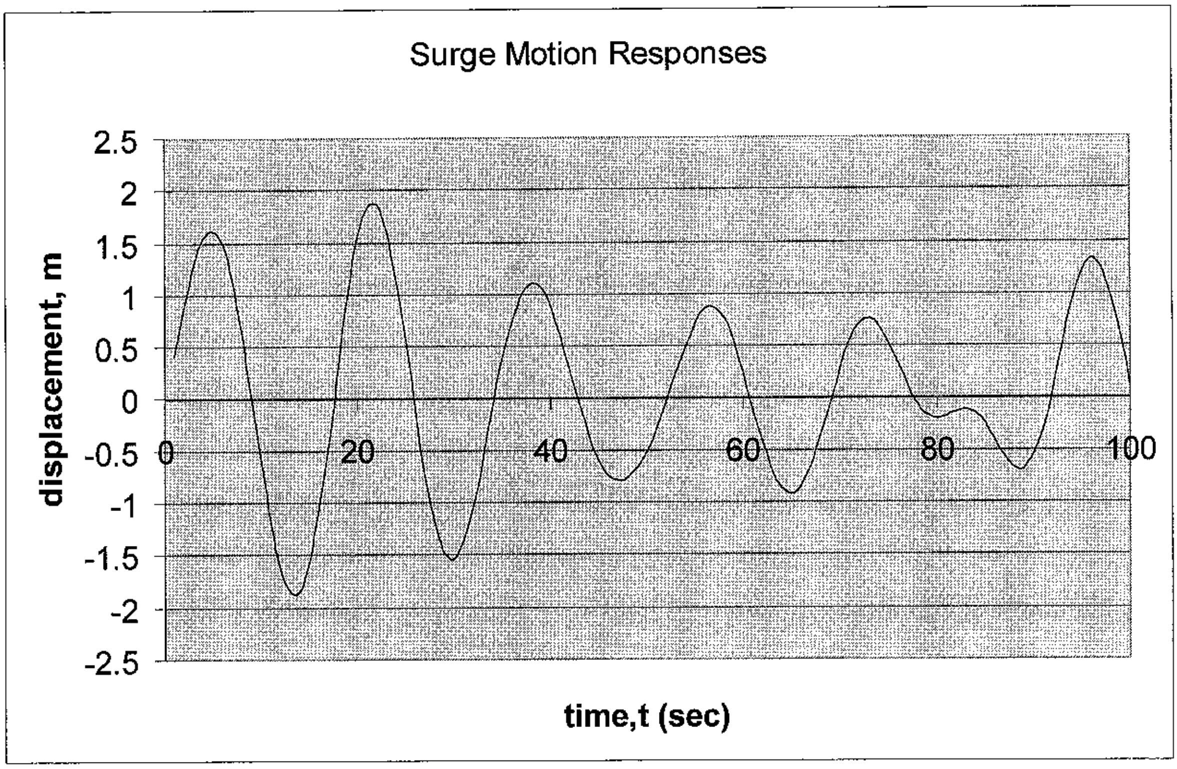

Graph 5: Surge displacement versus time, t.

Surge is defined by horizontal movement of the spar platform. The magnitudes of the movement basically govern by the motion response of the system. The motion response consists of various parameter such as force, total mass and stiffness. From the result, the spar platform move backward 1.7m which is the maximum value. For spar platform, it consider stable as spar structure allow certain limit of movement compare to tension leg platform.

- **RAO for Heave**

$$RAO = \left[\frac{F_I/(H/2)}{\left[(K - m\omega^2)^2 + (C\omega^2) \right]^{1/2}} \right]$$

Table 10 : **RAO parameter details**

T spar	30	sec
Hs	10.7	m
K, stiffness	10980079.11	N/m
m	221655000	kg
m(added)	13883244.72	kg
Mtotal	235538244.7	kg
ς	0.02	
C	1973496.44	
D	37.2	m
ρ (density)	1030	kg/m³
g (gravity)	9.807	m/sec²
Draft	198	m

Table 11: RAO heave calculation

Total force (N)	Frequency	S(*f*)	H	RAO	RAO²
170465.4783	0.035	0.084636067	0.08228539	0.387520056	0.150171794
1910937.462	0.045	38.38685069	1.752412068	0.207637899	0.043113497
1681699.53	0.055	147.384008	3.433761879	0.095392896	0.009099805
673460.7901	0.065	161.9469516	3.599410525	0.037474001	0.001404301
189170.3013	0.075	121.2497386	3.114478943	0.012580164	0.000158261
42491.03666	0.085	80.58194193	2.539006765	0.003606811	1.30091E-05
7979.216432	0.095	52.10202572	2.041607714	0.0008826	7.78983E-07
1.646861485	0.105	33.9019094	1.646861485	2.38498E-07	5.68811E-14
172.8973126	0.115	22.47507469	1.340897451	3.27747E-05	1.07418E-09
20.030989	0.125	15.23807251	1.104104071	4.9678E-06	2.4679E-11
1.973220192	0.135	10.56907523	0.919524887	6.4127E-07	4.11227E-13
0.164660891	0.145	7.49098212	0.774130848	7.0494E-08	4.9694E-15
0.011584414	0.155	5.41670036	0.658282636	6.60328E-09	4.36033E-17
0.000682991	0.165	3.989136843	0.564916762	5.28051E-10	2.78838E-19
3.34812E-05	0.175	2.987121188	0.488845267	3.62141E-11	1.31146E-21
1.34977E-06	0.185	2.270884552	0.426228535	2.15314E-12	4.63603E-24
4.39977E-08	0.195	1.750286931	0.374196412	1.14154E-13	1.30312E-26
1.12532E-09	0.205	1.366039806	0.330580073	5.89567E-15	3.47589E-29
2.11402E-11	0.215	1.078412146	0.29372261	3.31499E-16	1.09891E-31
2.33593E-13	0.225	0.86030858	0.262344595	1.70697E-18	2.91374E-36
-8.86265E-16	0.235	0.692946438	0.235447903	-3.61959E-21	1.31014E-41
-1.06616E-16	0.245	0.563105951	0.212246263	-3.14454E-22	9.8881E-44
-2.66644E-18	0.255	0.461350184	0.192114588	-6.35955E-24	4.04439E-47
-4.18311E-20	0.265	0.380853422	0.174551636	-8.58166E-26	7.3645E-51
-4.55985E-22	0.275	0.316617857	0.159152218	-8.36031E-28	6.98948E-55

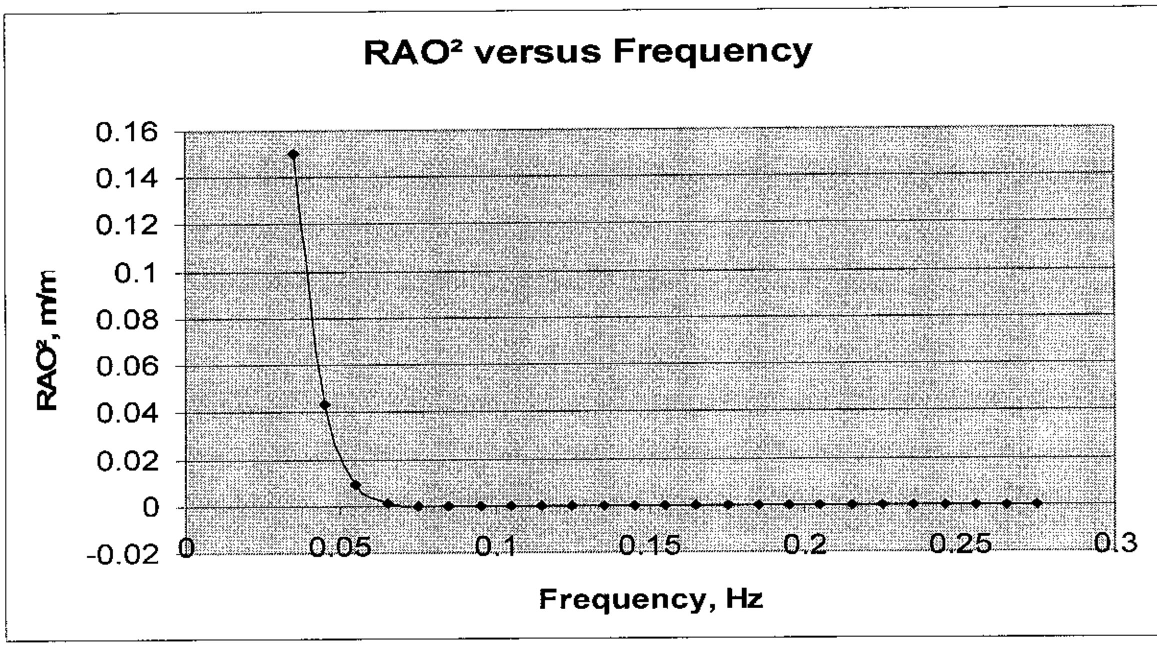

Graph 6: RAO² heave versus frequency.

- **S heave response spectrum**

$$S_{(f)Heave} = RAO^2_{heave} * S(f)_{wave}$$

Table 12 : S heave spectrum calculation

frequency	S(f)	RAO²	S Heave
0.035	0.084636067	0.150171794	0.01270995
0.045	38.38685069	0.043113497	1.654991369
0.055	147.384008	0.009099805	1.341165686
0.065	161.9469516	0.001404301	0.227422228
0.075	121.2497386	0.000158261	0.019189048
0.085	80.58194193	1.30091E-05	0.001048297
0.095	52.10202572	7.78983E-07	4.05866E-05
0.105	33.9019094	5.68811E-14	1.92838E-12
0.115	22.47507469	1.07418E-09	2.41423E-08
0.125	15.23807251	2.4679E-11	3.76061E-10
0.135	10.56907523	4.11227E-13	4.34629E-12
0.145	7.49098212	4.9694E-15	3.72257E-14
0.155	5.41670036	4.36033E-17	2.36186E-16
0.165	3.989136843	2.78838E-19	1.11232E-18
0.175	2.987121188	1.31146E-21	3.91749E-21
0.185	2.270884552	4.63603E-24	1.05279E-23
0.195	1.750286931	1.30312E-26	2.28084E-26
0.205	1.366039806	3.47589E-29	4.7482E-29
0.215	1.078412146	1.09891E-31	1.18508E-31
0.225	0.86030858	2.91374E-36	2.50671E-36
0.235	0.692946438	1.31014E-41	9.07859E-42
0.245	0.563105951	9.8881E-44	5.56805E-44
0.255	0.461350184	4.04439E-47	1.86588E-47
0.265	0.380853422	7.3645E-51	2.80479E-51
0.275	0.316617857	6.98948E-55	2.213E-55

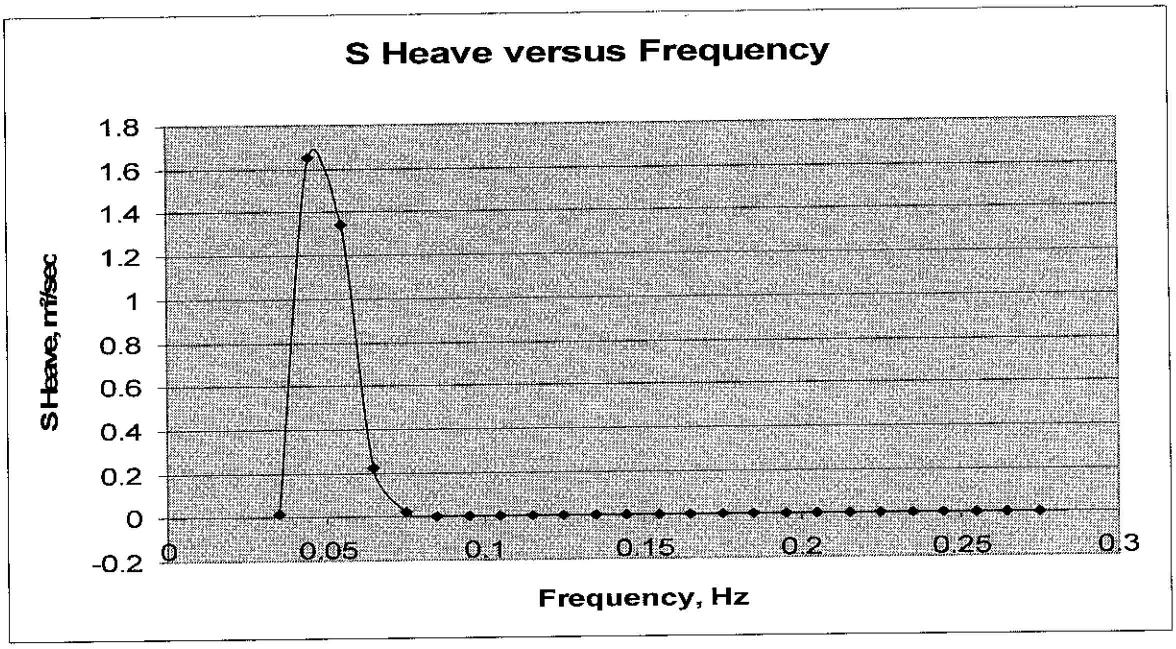

Graph 7: S heave spectrum

- **Heave Responses Profile**

Table 13: Heave responses profile calculation

t	f	f(n)	S(f)	H(f)	Rn	ε(n)	$\frac{H(n)}{2}\cos[k(n)x - 2\pi f(n)t + \varepsilon(n)]$
1	f1	0.035	0.01271	0.031887	0.324517	2.039268	-0.003921824
1	f2	0.045	1.654991	0.363867	0.782798	4.9191	-0.013826144
1	f3	0.055	1.341166	0.327556	0.133234	0.837245	0.144381449
1	f4	0.065	0.227422	0.134884	0.07188	0.451696	0.067379131
1	f5	0.075	0.019189	0.039181	0.255017	1.602529	0.008336632
1	f6	0.085	0.001048	0.009158	0.560611	3.522881	-0.004525473
1	f7	0.095	4.06E-05	0.001802	0.19634	1.233799	0.000724366
1	f8	0.105	1.93E-12	3.93E-07	0.921712	5.792037	8.00478E-08
1	f9	0.115	2.41E-08	4.39E-05	0.712048	4.474512	-1.80075E-05
1	f10	0.125	3.76E-10	5.48E-06	0.861061	5.410904	-2.38253E-07
1	f11	0.135	4.35E-12	5.9E-07	0.787032	4.945709	-1.7011E-07
1	f12	0.145	3.72E-14	5.46E-08	0.916729	5.760726	3.73072E-09
1	f13	0.155	2.36E-16	4.35E-09	0.852886	5.359535	-6.97848E-10
1	f14	0.165	1.11E-18	2.98E-10	0.952698	5.986752	3.50921E-11
1	f15	0.175	3.92E-21	1.77E-11	0.54218	3.407056	-5.94597E-12
1	f16	0.185	1.05E-23	9.18E-13	0.86603	5.442132	-1.92454E-13
1	f17	0.195	2.28E-26	4.27E-14	0.421035	2.645782	3.20005E-15
1	f18	0.205	4.75E-29	1.95E-15	0.16736	1.051688	9.47362E-16
1	f19	0.215	1.19E-31	9.74E-17	0.398134	2.501873	1.98508E-17
1	f20	0.225	2.51E-36	4.48E-19	0.34	2.136561	1.67941E-19
1	f21	0.235	9.08E-42	8.52E-22	0.474881	2.984151	2.69911E-23
1	f22	0.245	5.57E-44	6.67E-23	0.533067	3.34979	-7.91332E-24
1	f23	0.255	1.87E-47	1.22E-24	0.495259	3.112211	3.72442E-26
1	f24	0.265	2.8E-51	1.5E-26	0.419311	2.634952	4.23584E-27
1	f25	0.275	2.21E-55	1.33E-28	0.250598	1.574759	6.57475E-29
						n(x,t)	0.198529804

***t is varied from 1 to 100**

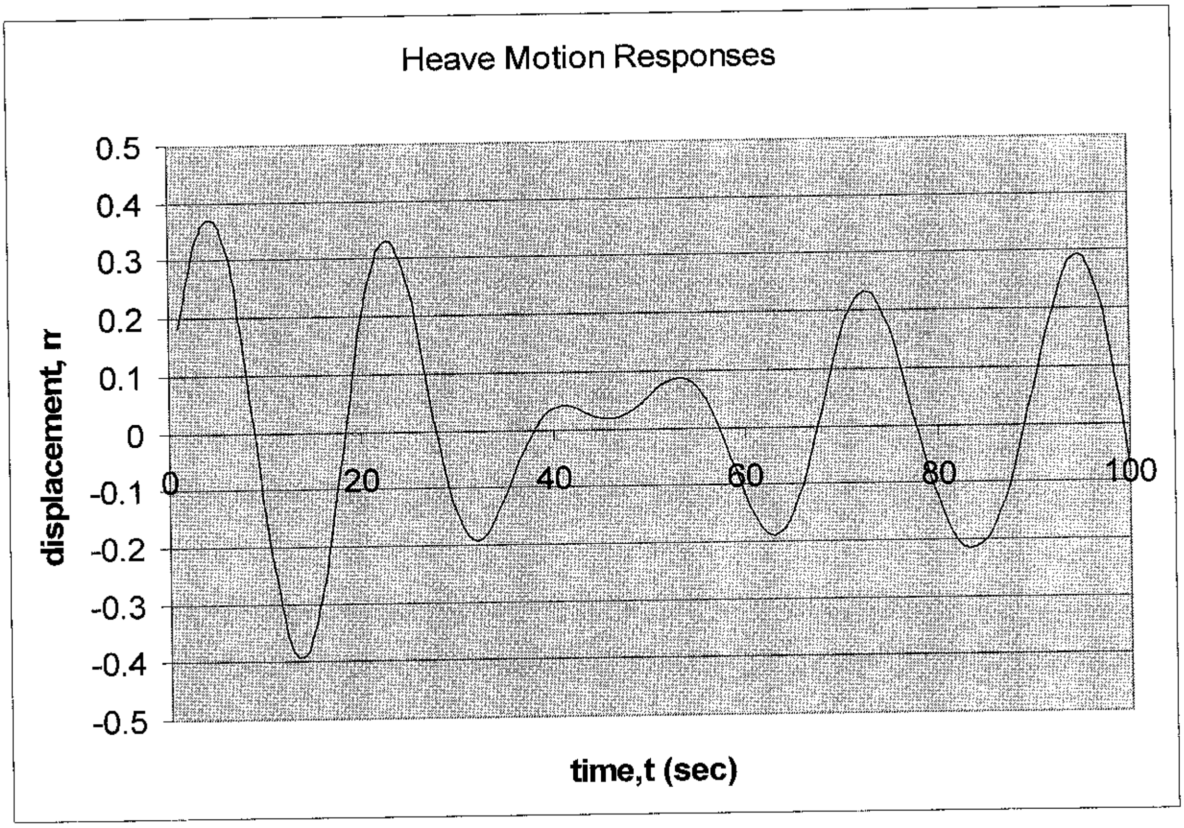

Graph 8: Heave elevation versus time, t.

Heave is defined by vertical movement of the spar platform. The magnitudes of the movement basically govern by the motion response of the system. The motion response consists of various parameter such as force, total mass and stiffness. From the result, the spar platform move downward 5.7m which is the maximum value. For spar platform, it consider stable as spar structure allow certain limit of movement compare to tension leg platform.

- RAO for Pitch

$$RAO = \left[\frac{M_I/(H/2)}{\left[(K - I\omega^2)^2 + (C\omega)^2\right]^{1/2}} \right]$$

Table 14: RAO pitch calculation

Total Moment (M)	Frequency	S(*f*)	H	RAO	RAO²
-683.152165	0.035	0.084636	0.08228539	-8.1E-07	6.53108E-13
-1103777.284	0.045	38.38685	1.752412068	-6.1E-05	3.75881E-09
-7058197.251	0.055	147.384	3.433761879	-0.0002	4.00253E-08
-10075707.61	0.065	161.947	3.599410525	-0.00027	7.42183E-08
-8757118.172	0.075	121.2497	3.114478943	-0.00027	7.48684E-08
-6391066.518	0.085	80.58194	2.539006765	-0.00024	5.99901E-08
-4406264.521	0.095	52.10203	2.041607714	-0.00021	4.4092E-08
-3006432.391	0.105	33.90191	1.646861485	-0.00018	3.15388E-08
-2068930.611	0.115	22.47507	1.340897451	-0.00015	2.25236E-08
-1446821.511	0.125	15.23807	1.104104071	-0.00013	1.62412E-08
-1030748.357	0.135	10.56908	0.919524887	-0.00011	1.18808E-08
-748318.1747	0.145	7.490982	0.774130848	-9.4E-05	8.83204E-09
-553244.4209	0.155	5.4167	0.658282636	-8.2E-05	6.67367E-09
-416075.453	0.165	3.989137	0.564916762	-7.2E-05	5.12341E-09
-317924.7524	0.175	2.987121	0.488845267	-6.3E-05	3.99307E-09
-246518.1502	0.185	2.270885	0.426228535	-5.6E-05	3.1566E-09
-193753.1255	0.195	1.750287	0.374196412	-5E-05	2.52872E-09
-154193.0554	0.205	1.36604	0.330580073	-4.5E-05	2.05099E-09
-124130.6154	0.215	1.078412	0.29372261	-4.1E-05	1.68285E-09
-100997.8973	0.225	0.860309	0.262344595	-3.7E-05	1.39575E-09
-82989.52662	0.235	0.692946	0.235447903	-3.4E-05	1.16933E-09
-68818.2254	0.245	0.563106	0.212246263	-3.1E-05	9.88893E-10
-57553.87866	0.255	0.46135	0.192114588	-2.9E-05	8.4369E-10
-48516.01246	0.265	0.380853	0.174551636	-2.7E-05	7.25769E-10
-41200.93552	0.275	0.316618	0.159152218	-2.5E-05	6.29182E-10

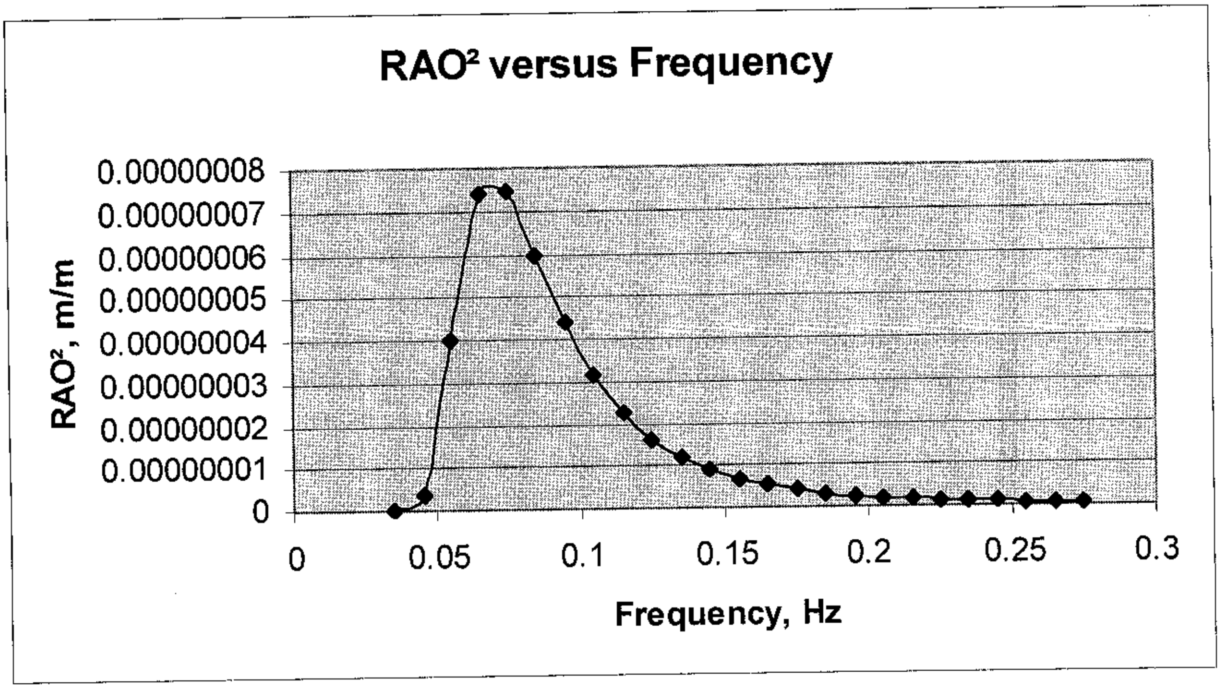

Graph 9: RAO pitch versus Frequency

- **S Pitch Response Spectrum**

$$S_{(f)Pitch} = RAO_{pitch}^{2} * S(f)_{wave}$$

Table 15: S pitch spectrum calculation

frequency	S(f)	RAO²	S pitch
0.035	0.084636067	6.53108E-13	5.52765E-14
0.045	38.38685069	3.75881E-09	1.44289E-07
0.055	147.384008	4.00253E-08	5.89909E-06
0.065	161.9469516	7.42183E-08	1.20194E-05
0.075	121.2497386	7.48684E-08	9.07778E-06
0.085	80.58194193	5.99901E-08	4.83412E-06
0.095	52.10202572	4.4092E-08	2.29728E-06
0.105	33.9019094	3.15388E-08	1.06922E-06
0.115	22.47507469	2.25236E-08	5.0622E-07
0.125	15.23807251	1.62412E-08	2.47484E-07
0.135	10.56907523	1.18808E-08	1.25569E-07
0.145	7.49098212	8.83204E-09	6.61606E-08
0.155	5.41670036	6.67367E-09	3.61493E-08
0.165	3.989136843	5.12341E-09	2.0438E-08
0.175	2.987121188	3.99307E-09	1.19278E-08
0.185	2.270884552	3.1566E-09	7.16828E-09
0.195	1.750286931	2.52872E-09	4.42599E-09
0.205	1.366039806	2.05099E-09	2.80174E-09
0.215	1.078412146	1.68285E-09	1.81481E-09
0.225	0.86030858	1.39575E-09	1.20077E-09
0.235	0.692946438	1.16933E-09	8.10282E-10
0.245	0.563105951	9.88893E-10	5.56851E-10
0.255	0.461350184	8.4369E-10	3.89237E-10
0.265	0.380853422	7.25769E-10	2.76412E-10
0.275	0.316617857	6.29182E-10	1.9921E-10

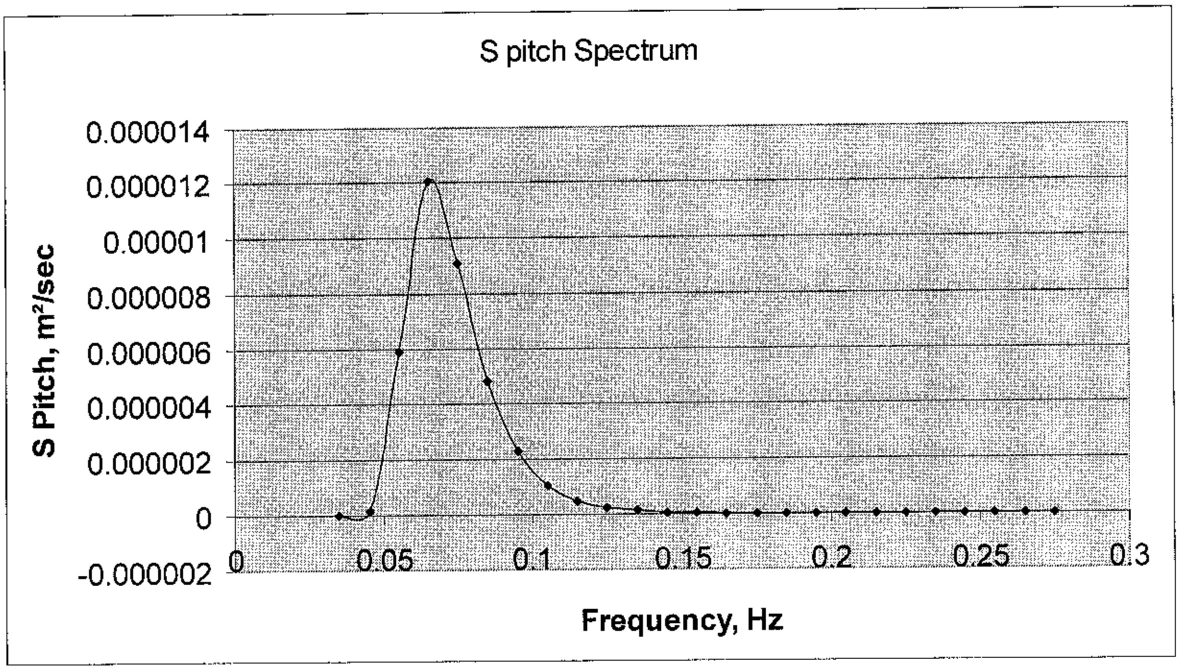

Graph 10: S Pitch Spectrum

- **Pitch Responses Profile**

Table 16: Pitch responses profile calculation

t	f	f(n)	S(f)	H(f)	Rn	ε(n)	$\frac{H(n)}{2}\cos[k(n)x - 2\pi f(n)t + \varepsilon(n)]$
1	f1	0.035	5.53E-14	6.65E-08	0.860315	5.406217	1.51734E-08
1	f2	0.045	1.44E-07	0.000107	0.761549	4.785575	-1.1177E-05
1	f3	0.055	5.9E-06	0.000687	0.378085	2.375888	-0.000152327
1	f4	0.065	1.2E-05	0.000981	0.733758	4.610936	-0.000239313
1	f5	0.075	9.08E-06	0.000852	0.020672	0.129903	0.000401503
1	f6	0.085	4.83E-06	0.000622	0.397689	2.499076	-0.000119404
1	f7	0.095	2.3E-06	0.000429	0.767971	4.825928	-9.96358E-05
1	f8	0.105	1.07E-06	0.000292	0.651587	4.094575	-0.000139995
1	f9	0.115	5.06E-07	0.000201	0.175791	1.104669	9.33671E-05
1	f10	0.125	2.47E-07	0.000141	0.033299	0.209253	5.89928E-05
1	f11	0.135	1.26E-07	0.0001	0.794763	4.994293	-2.68924E-05
1	f12	0.145	6.62E-08	7.28E-05	0.53518	3.363072	-2.80618E-05
1	f13	0.155	3.61E-08	5.38E-05	0.159995	1.005408	2.68751E-05
1	f14	0.165	2.04E-08	4.04E-05	0.850335	5.343507	-7.97998E-06
1	f15	0.175	1.19E-08	3.09E-05	0.69924	4.394024	-1.52654E-05
1	f16	0.185	7.17E-09	2.39E-05	0.673305	4.231052	-1.19416E-05
1	f17	0.195	4.43E-09	1.88E-05	0.943416	5.928424	-8.7925E-08
1	f18	0.205	2.8E-09	1.5E-05	0.425238	2.672195	1.39036E-06
1	f19	0.215	1.81E-09	1.2E-05	0.421208	2.646872	1.63588E-06
1	f20	0.225	1.2E-09	9.8E-06	0.096773	0.608124	3.39389E-06
1	f21	0.235	8.1E-10	8.05E-06	0.112271	0.705511	2.88659E-06
1	f22	0.245	5.57E-10	6.67E-06	0.232771	1.462735	3.32737E-06
1	f23	0.255	3.89E-10	5.58E-06	0.792764	4.981731	-2.71165E-06
1	f24	0.265	2.76E-10	4.7E-06	0.169537	1.065371	1.94069E-06
1	f25	0.275	1.99E-10	3.99E-06	0.207177	1.3019	1.81749E-06
						n(x,t)	-0.000257648

*t varies from 1 to 100 seconds

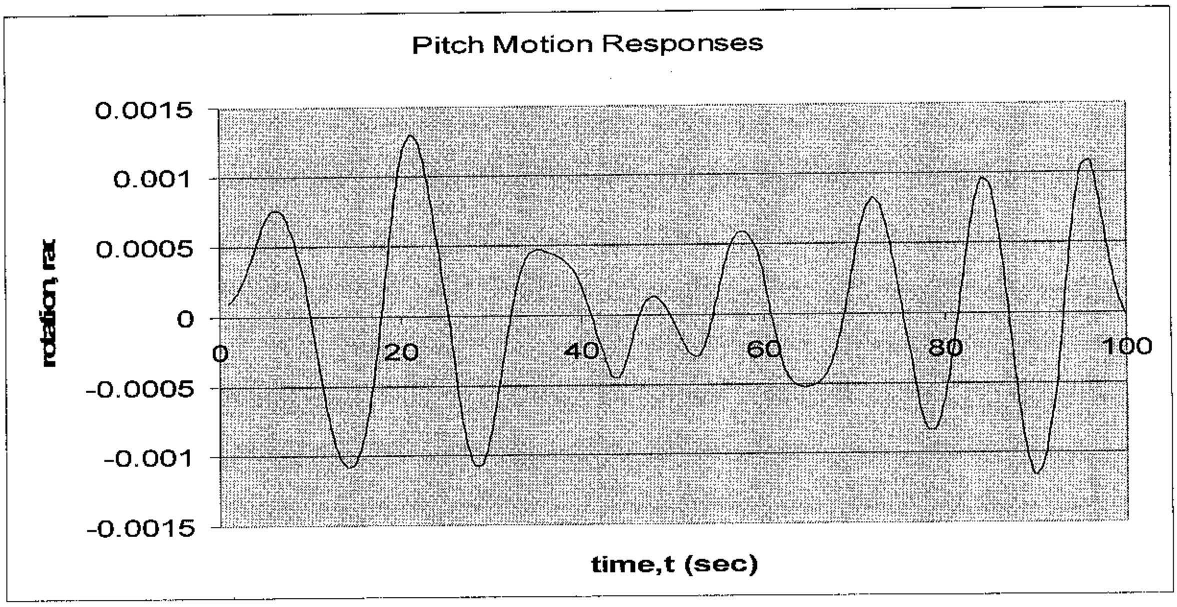

Graph 11: Pitch rotation versus time,t.

Pitch is defined by rotation of the spar platform. The magnitudes of the rotation basically govern by the motion response of the system. The motion response consists of various parameter such as force, moment, total mass and stiffness. From the result, the spar platform rotates 0.086 degree which is its maximum rotation. For spar platform, it consider stable as spar structure allow certain limit of rotation.

4.6 Analysis on Parametric Studies

For final research of this project which is parametric studies, five water depths including the original data has been chosen. This value is chosen base on the current water depth which cover from the shallowest to deepest depth spar platform has been installed. The four water depth chosen are 492, 792, 1092, 1392, 1692 meters depth.

Calculation has been made for all motion responses for all water depth where it has been found that water depth will not affect the responses as long as the depth of the water fall into deep water situation. For all spar platforms, the field location is located in deep water region.

Calculation for responses factor, RAO for all water depths provide same results and values. In deep water, wave length does not affect by water depth where:

$$L = {gT^2}/{2\pi}$$

Where:

g = gravity acceleration

T = wave period

From wave length value, k is calculated where it's needed to calculate water particle velocity. k is given by:

$$k = {L}/{2\pi}$$

Where:

L = wave length

With k constant for all water depths, water particle velocities give the same values and affect the same values for force and moment. As a result, RAO values are the same as well as motion response.

- Surge motion responses for various water depth

Table 17: Surge RAO² result for various water depths

	RAO²				
frequency	492m	792m	1092m	1392m	1692m
0.035	0.000173364	0.000157306	0.000156513	0.000156472	0.00015647
0.045	0.044499742	0.044243174	0.044241255	0.044241241	0.044241241
0.055	0.349096257	0.349041147	0.34904111	0.34904111	0.34904111
0.065	0.125788977	0.125788684	0.125788684	0.125788684	0.125788684
0.075	0.028501571	0.02850157	0.02850157	0.02850157	0.02850157
0.085	0.007946123	0.007946123	0.007946123	0.007946123	0.007946123
0.095	0.002628316	0.002628316	0.002628316	0.002628316	0.002628316
0.105	0.000990932	0.000990932	0.000990932	0.000990932	0.000990932
0.115	0.000414389	0.000414389	0.000414389	0.000414389	0.000414389
0.125	0.000188535	0.000188535	0.000188535	0.000188535	0.000188535
0.135	9.20048E-05	9.20048E-05	9.20048E-05	9.20048E-05	9.20048E-05
0.145	4.76374E-05	4.76374E-05	4.76374E-05	4.76374E-05	4.76374E-05
0.155	2.59492E-05	2.59492E-05	2.59492E-05	2.59492E-05	2.59492E-05
0.165	1.4771E-05	1.4771E-05	1.4771E-05	1.4771E-05	1.4771E-05
0.175	8.73843E-06	8.73843E-06	8.73843E-06	8.73843E-06	8.73843E-06
0.185	5.34873E-06	5.34873E-06	5.34873E-06	5.34873E-06	5.34873E-06
0.195	3.37477E-06	3.37477E-06	3.37477E-06	3.37477E-06	3.37477E-06
0.205	2.18806E-06	2.18806E-06	2.18806E-06	2.18806E-06	2.18806E-06
0.215	1.45392E-06	1.45392E-06	1.45392E-06	1.45392E-06	1.45392E-06
0.225	9.8788E-07	9.8788E-07	9.8788E-07	9.8788E-07	9.8788E-07
0.235	6.85012E-07	6.85012E-07	6.85012E-07	6.85012E-07	6.85012E-07
0.245	4.83931E-07	4.83931E-07	4.83931E-07	4.83931E-07	4.83931E-07
0.255	3.47785E-07	3.47785E-07	3.47785E-07	3.47785E-07	3.47785E-07
0.265	2.53927E-07	2.53927E-07	2.53927E-07	2.53927E-07	2.53927E-07
0.275	1.88136E-07	1.88136E-07	1.88136E-07	1.88136E-07	1.88136E-07

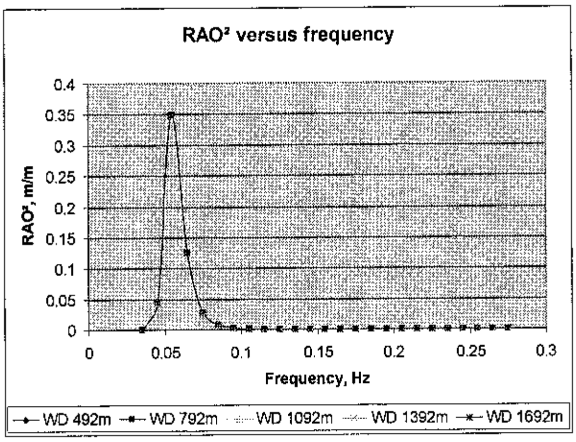

Graph 12: Surge RAO² for various water depths

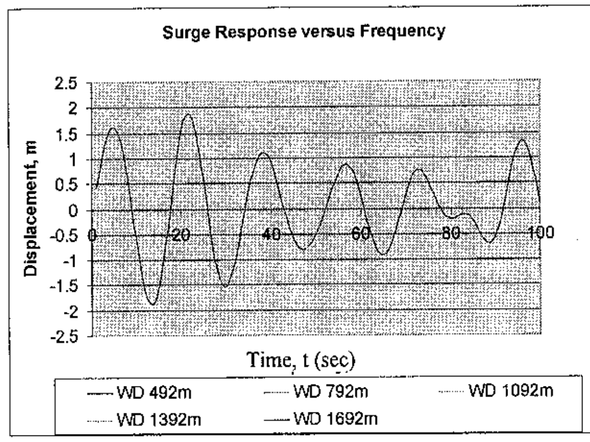

Graph 13: Surge responses for various water depths

- Heave motion responses for various water depth

Table 18: Heave RAO² result for various water depths

	RAO²				
Frequency	492m	792m	1092m	1392m	1692m
0.035	0.150171402	0.150171402	0.150171402	0.150171402	0.150171402
0.045	0.043113304	0.043113304	0.043113304	0.043113304	0.043113304
0.055	0.009099741	0.009099741	0.009099741	0.009099741	0.009099741
0.065	0.001404286	0.001404286	0.001404286	0.001404286	0.001404286
0.075	0.000158258	0.000158258	0.000158258	0.000158258	0.000158258
0.085	1.30088E-05	1.30088E-05	1.30088E-05	1.30088E-05	1.30088E-05
0.095	7.78962E-07	7.78962E-07	7.78962E-07	7.78962E-07	7.78962E-07
0.105	5.68789E-14	5.68789E-14	5.68789E-14	5.68789E-14	5.68789E-14
0.115	1.07412E-09	1.07412E-09	1.07412E-09	1.07412E-09	1.07412E-09
0.125	2.46773E-11	2.46773E-11	2.46773E-11	2.46773E-11	2.46773E-11
0.135	4.11186E-13	4.11186E-13	4.11186E-13	4.11186E-13	4.11186E-13
0.145	4.96871E-15	4.96871E-15	4.96871E-15	4.96871E-15	4.96871E-15
0.155	4.35943E-17	4.35943E-17	4.35943E-17	4.35943E-17	4.35943E-17
0.165	2.7875E-19	2.7875E-19	2.7875E-19	2.7875E-19	2.7875E-19
0.175	1.31078E-21	1.31078E-21	1.31078E-21	1.31078E-21	1.31078E-21
0.185	4.63157E-24	4.63157E-24	4.63157E-24	4.63157E-24	4.63157E-24
0.195	1.30029E-26	1.30029E-26	1.30029E-26	1.30029E-26	1.30029E-26
0.205	3.44944E-29	3.44944E-29	3.44944E-29	3.44944E-29	3.44944E-29
0.215	1.03706E-31	1.03706E-31	1.03706E-31	1.03706E-31	1.03706E-31
0.225	2.88113E-36	2.88113E-36	2.88113E-36	2.88113E-36	2.88113E-36
0.235	1.30609E-41	1.30609E-41	1.30609E-41	1.30609E-41	1.30609E-41
0.245	9.87397E-44	9.87397E-44	9.87397E-44	9.87397E-44	9.87397E-44
0.255	4.04103E-47	4.04103E-47	4.04103E-47	4.04103E-47	4.04103E-47
0.265	7.36046E-51	7.36046E-51	7.36046E-51	7.36046E-51	7.36046E-51
0.275	6.98675E-55	6.98675E-55	6.98675E-55	6.98675E-55	6.98675E-55

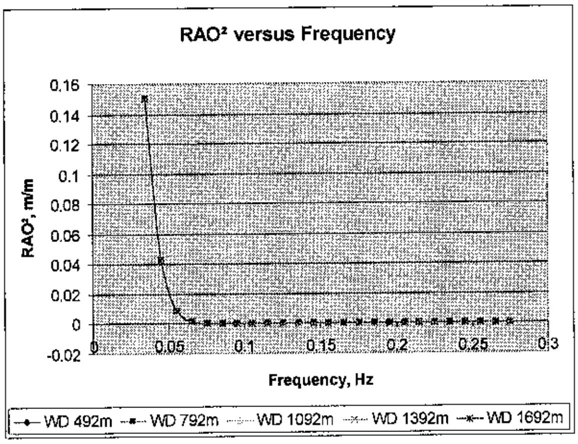

Graph 14: Heave RAO² for various water depths

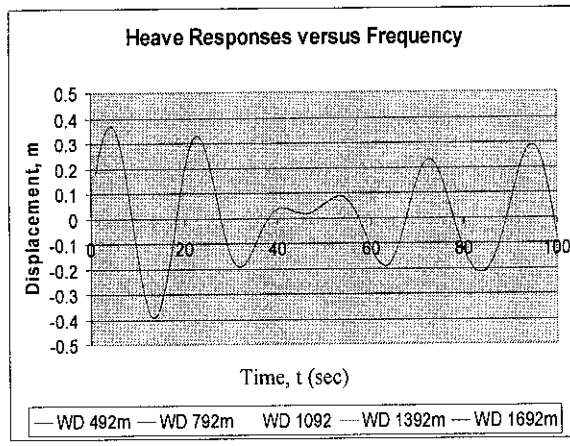

Graph 15: Heave responses for various water depths

- Pitch motion responses for various water depths

Table 19: Pitch RAO² result for various water depths

	RAO²				
Frequency	492m	792m	1092m	1392m	1692m
0.035	5.27324E-13	6.53108E-13	6.59679E-13	6.60019E-13	6.60037E-13
0.045	3.74599E-09	3.75881E-09	3.75891E-09	3.75891E-09	3.75891E-09
0.055	4.00227E-08	4.00253E-08	4.00253E-08	4.00253E-08	4.00253E-08
0.065	7.42182E-08	7.42183E-08	7.42183E-08	7.42183E-08	7.42183E-08
0.075	7.48684E-08	7.48684E-08	7.48684E-08	7.48684E-08	7.48684E-08
0.085	5.99901E-08	5.99901E-08	5.99901E-08	5.99901E-08	5.99901E-08
0.095	4.4092E-08	4.4092E-08	4.4092E-08	4.4092E-08	4.4092E-08
0.105	3.15388E-08	3.15388E-08	3.15388E-08	3.15388E-08	3.15388E-08
0.115	2.25236E-08	2.25236E-08	2.25236E-08	2.25236E-08	2.25236E-08
0.125	1.62412E-08	1.62412E-08	1.62412E-08	1.62412E-08	1.62412E-08
0.135	1.18808E-08	1.18808E-08	1.18808E-08	1.18808E-08	1.18808E-08
0.145	8.83204E-09	8.83204E-09	8.83204E-09	8.83204E-09	8.83204E-09
0.155	6.67367E-09	6.67367E-09	6.67367E-09	6.67367E-09	6.67367E-09
0.165	5.12341E-09	5.12341E-09	5.12341E-09	5.12341E-09	5.12341E-09
0.175	3.99307E-09	3.99307E-09	3.99307E-09	3.99307E-09	3.99307E-09
0.185	3.1566E-09	3.1566E-09	3.1566E-09	3.1566E-09	3.1566E-09
0.195	2.52872E-09	2.52872E-09	2.52872E-09	2.52872E-09	2.52872E-09
0.205	2.05099E-09	2.05099E-09	2.05099E-09	2.05099E-09	2.05099E-09
0.215	1.68285E-09	1.68285E-09	1.68285E-09	1.68285E-09	1.68285E-09
0.225	1.39575E-09	1.39575E-09	1.39575E-09	1.39575E-09	1.39575E-09
0.235	1.16933E-09	1.16933E-09	1.16933E-09	1.16933E-09	1.16933E-09
0.245	9.88893E-10	9.88893E-10	9.88893E-10	9.88893E-10	9.88893E-10
0.255	8.4369E-10	8.4369E-10	8.4369E-10	8.4369E-10	8.4369E-10
0.265	7.25769E-10	7.25769E-10	7.25769E-10	7.25769E-10	7.25769E-10
0.275	6.29182E-10	6.29182E-10	6.29182E-10	6.29182E-10	6.29182E-10

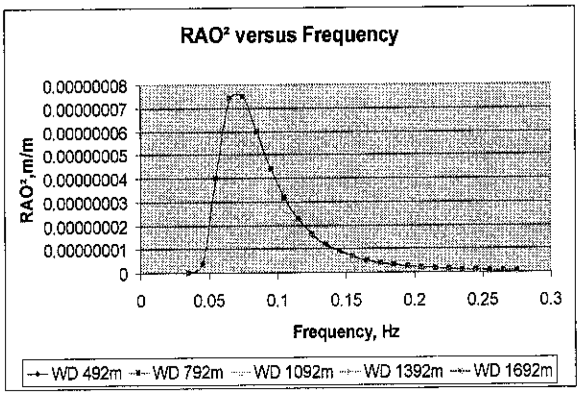

Graph 16: Pitch RAO² for various water depths

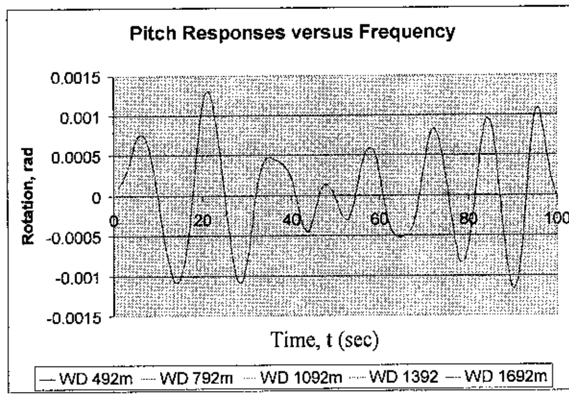

Graph 17: Pitch responses for various water depths

From the results shown, it is proven than the water depth is not matter to the behaviour of spar platform. It gives same result to the motion response even though the different between the depths are large.

4.7 Analysis on Drag and Mass Coefficient for Tubular Member

Drag and mass coefficient Cd and Cm are taken into account in calculating wave force. The coefficient is determined by the condition of the tubular member. For instance, in this research, three combinations of Cd and Cm are chosen. The combinations are:

1. Typical member (Cd = 0.7, Cm = 2)
2. Clean member (Cd = 0.65, Cm = 1.6)
3. Fouled member (Cd = 1.05, Cm = 1.2)

In this analysis, all the data are remain the same except for drag and mass coefficient to see the effect and the different.

- Surge motion responses for various combination of drag and mass coefficient

Table 20: Surge RAO² result for various combination of drag and mass coefficient

	RAO²		
	typical member	clean member	fouled member
frequency	Cd = 0.7, Cm = 2	Cd = 0.65, Cm = 1.6	Cd = 1.05, Cm = 1.2
0.035	0.000157306	0.000135636	0.000353938
0.045	0.044243174	0.038148451	0.099547141
0.055	0.349041147	0.300958948	0.785342581
0.065	0.125788684	0.108460651	0.283024539
0.075	0.02850157	0.024575333	0.064128532
0.085	0.007946123	0.006851504	0.017878776
0.095	0.002628316	0.002266252	0.005913711
0.105	0.000990932	0.000854426	0.002229596
0.115	0.000414389	0.000357305	0.000932376
0.125	0.000188535	0.000162564	0.000424204
0.135	9.20048E-05	7.93307E-05	0.000207011
0.145	4.76374E-05	4.10751E-05	0.000107184
0.155	2.59492E-05	2.23746E-05	5.83857E-05
0.165	1.4771E-05	1.27362E-05	3.32347E-05
0.175	8.73843E-06	7.53466E-06	1.96615E-05
0.185	5.34873E-06	4.61191E-06	1.20346E-05
0.195	3.37477E-06	2.90988E-06	7.59324E-06
0.205	2.18806E-06	1.88664E-06	4.92313E-06
0.215	1.45392E-06	1.25364E-06	3.27132E-06
0.225	9.8788E-07	8.51794E-07	2.22273E-06
0.235	6.85012E-07	5.90648E-07	1.54128E-06
0.245	4.83931E-07	4.17267E-07	1.08884E-06
0.255	3.47785E-07	2.99876E-07	7.82516E-07
0.265	2.53927E-07	2.18948E-07	5.71336E-07
0.275	1.88136E-07	1.6222E-07	4.23307E-07

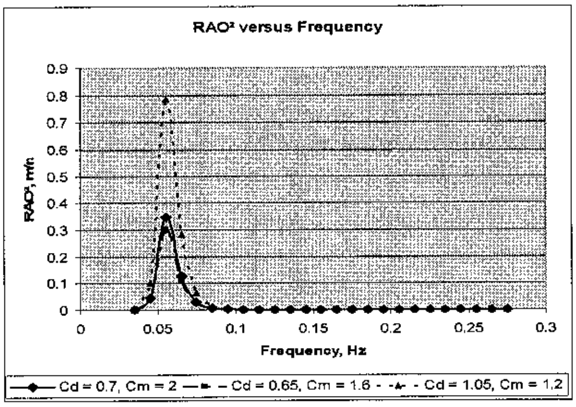

Graph 18: Surge RAO² for various Cd and Cm

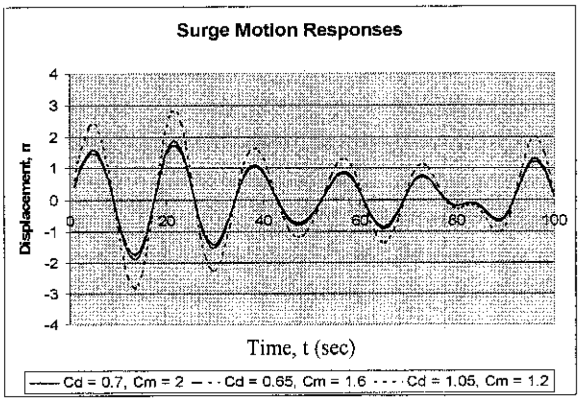

Graph 19: Surge responses for various Cd and Cm

Refer to the Surge RAO² graph, drag and mass coefficient value give significant differences. From observation, clean member produce little lower value where fouled member produce higher response factor compare with typical member. This is expected result since the coefficient is used in calculating force.

For the motion responses, fouled member drag and mass coefficient give the highest value where 2.8 meters horizontal movement where clean member coefficient give only 1.8 meters. This is due to response factor result for respective coefficient in previous graphs.

- Heave motion responses for various combination of drag and mass coefficient

Table 21: Heave RAO² result for various combination of drag and mass coefficient

	RAO²		
	typical member	clean member	fouled member
Frequency	Cd = 0.7, Cm = 2	Cd = 0.65, Cm = 1.6	Cd = 1.05, Cm = 1.2
0.035	0.150171794	0.150171794	0.150171794
0.045	0.043113497	0.043113497	0.043113497
0.055	0.009099805	0.009099805	0.009099805
0.065	0.001404301	0.001404301	0.001404301
0.075	0.000158261	0.000158261	0.000158261
0.085	1.30091E-05	1.30091E-05	1.30091E-05
0.095	7.78983E-07	7.78983E-07	7.78983E-07
0.105	5.68811E-14	5.68811E-14	5.68811E-14
0.115	1.07418E-09	1.07418E-09	1.07418E-09
0.125	2.4679E-11	2.4679E-11	2.4679E-11
0.135	4.11227E-13	4.11227E-13	4.11227E-13
0.145	4.9694E-15	4.9694E-15	4.9694E-15
0.155	4.36033E-17	4.36033E-17	4.36033E-17
0.165	2.78838E-19	2.78838E-19	2.78838E-19
0.175	1.31146E-21	1.31146E-21	1.31146E-21
0.185	4.63603E-24	4.63603E-24	4.63603E-24
0.195	1.30312E-26	1.30312E-26	1.30312E-26
0.205	3.47589E-29	3.47589E-29	3.47589E-29
0.215	1.09891E-31	1.09891E-31	1.09891E-31
0.225	2.91374E-36	2.91374E-36	2.91374E-36
0.235	1.31014E-41	1.31014E-41	1.31014E-41
0.245	9.8881E-44	9.8881E-44	9.8881E-44
0.255	4.04439E-47	4.04439E-47	4.04439E-47
0.265	7.3645E-51	7.3645E-51	7.3645E-51
0.275	6.98948E-55	6.98948E-55	6.98948E-55

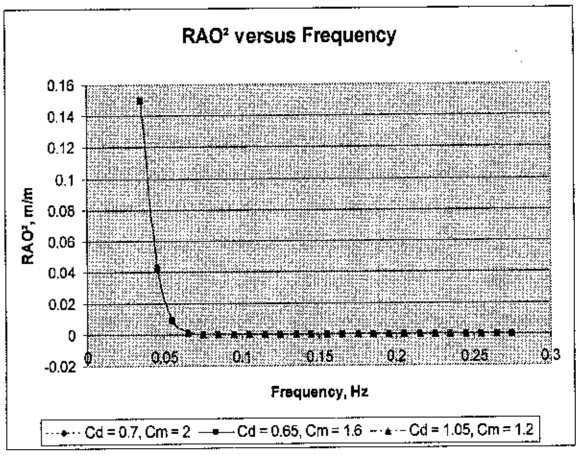

Graph 20: Heave RAO² for various Cd and Cm

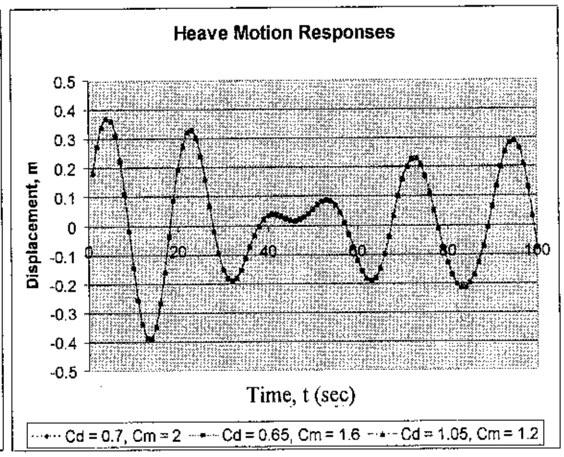

Graph 21: Heave responses for various Cd and Cm

Refer to the Heave RAO² graph above, drag and mass coefficient value give no significant differences. From observation, clean member produce same value with fouled member and typical member drag and mass coefficient. This is expected result since the coefficient is not used in calculating vertical force.

For the motion responses, all the coefficient give the highest value 0.38 meters vertical movement. This is due to response factor result for respective coefficient in previous graphs.

Refer to the pitch RAO² graph in next page, drag and mass coefficient value give significant differences. From observation, clean member produce little lower value where fouled member produce higher response factor compare with typical member. This is expected result since the coefficient is used in calculating force.

For the motion responses, fouled member drag and mass coefficient give the highest value where 0.002 rad rotation where clean member coefficient give only 0.0013 rad rotation. This is due to response factor results for respective coefficient in previous graphs.

- Pitch motion responses for various combination of drag and mass coefficient

Table 22: Pitch RAO² result for various combination of drag and mass coefficient

	RAO²		
	typical member	clean member	fouled member
Frequency	Cd = 0.7, Cm = 2	Cd = 0.65, Cm = 1.6	Cd = 1.05, Cm = 1.2
0.035	6.53108E-13	5.63139E-13	1.46949E-12
0.045	3.75881E-09	3.24102E-09	8.45733E-09
0.055	4.00253E-08	3.45116E-08	9.00569E-08
0.065	7.42183E-08	6.39943E-08	1.66991E-07
0.075	7.48684E-08	6.45549E-08	1.68454E-07
0.085	5.99901E-08	5.17262E-08	1.34978E-07
0.095	4.4092E-08	3.80181E-08	9.92071E-08
0.105	3.15388E-08	2.71941E-08	7.09622E-08
0.115	2.25236E-08	1.94209E-08	5.06781E-08
0.125	1.62412E-08	1.40039E-08	3.65427E-08
0.135	1.18808E-08	1.02442E-08	2.67318E-08
0.145	8.83204E-09	7.61538E-09	1.98721E-08
0.155	6.67367E-09	5.75434E-09	1.50158E-08
0.165	5.12341E-09	4.41763E-09	1.15277E-08
0.175	3.99307E-09	3.443E-09	8.9844E-09
0.185	3.1566E-09	2.72176E-09	7.10235E-09
0.195	2.52872E-09	2.18038E-09	5.68962E-09
0.205	2.05099E-09	1.76846E-09	4.61473E-09
0.215	1.68285E-09	1.45103E-09	3.78641E-09
0.225	1.39575E-09	1.20348E-09	3.14043E-09
0.235	1.16933E-09	1.00825E-09	2.63099E-09
0.245	9.88893E-10	8.52668E-10	2.22501E-09
0.255	8.4369E-10	7.27468E-10	1.8983E-09
0.265	7.25769E-10	6.25791E-10	1.63298E-09
0.275	6.29182E-10	5.42509E-10	1.41566E-09

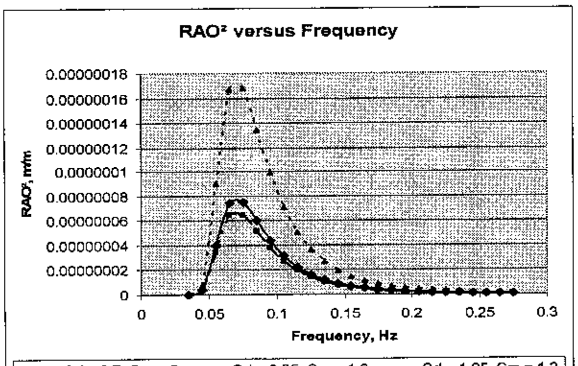

Graph 22: Pitch RAO² for various Cd and Cm

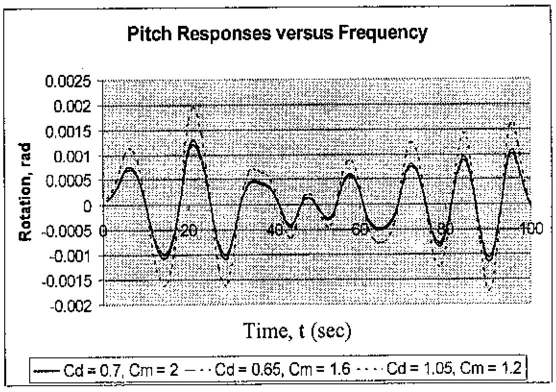

Graph 23: Pitch responses for various Cd and Cm

CHAPTER 5

CONCLUSION AND RECOMMENDATION

5.0 Conclusion and Recommendation

Spar is the most effective type of platform to be used in deep water exploration and production of oil and gas. Analysis of the structure and its response is beneficial for the designer to design better spar and reduce the cost also. This research help in analyzing spar platform on the effect of water depth

The calculation analysis shows that the water depth which fall in deep water region does not affect the motion responses.

From the analysis, it is conclude that mass and drag coefficient do give significant effect the motion of the spar platform based on the value.

It is recommended for further studies on effect of other parameter such as spar diameter or draft on its behaviour. This is importance for deep water structure stability and integrity development.

REFERENCE

1) Books
   a) Introduction to Offshore Structures *W.J. Graff*
   b) Offshore Engineering An Introduction *Angus Mather*
   c) Handbook of Offshore Engineering *chakrabarti*

2) Websites
   a) http://eprint.iitd.ac.in/dspace/bitstream/2074/1143/1/agarwaldyn2003.pdf
   b) http://www.aapg.org/explorer/2004/08aug/deepwater.cfm
   c) http://www.naturalgas.org/images/offshore_drill_platform.gif
   d) http://www.technip.com/english/pdf/SparProg
   e) http://www.globalsecurity.org/military/systems/ship/images/spars-image2.jpg

3) Journals
   a) J.M Niedzwecki and E.W Sandt "Characterizing the Excitation and Response of a Spar Buoy in Random sea".
   b) Edward G. Divis "A Spar Buoy Oceanographic Telemetry System".
   c) R. J. Lai, R. J. Bachman and E. W. Foley "Measurement of directional waves in finite water depth".
   d) Jeffrey V. Wilson and Dallas J. Meggitt "A survey spar system for precision offshore seafloor survey".
   e) W.M. Drennan, H.C Graber and M.A Donelan "Directional wave measurements from the ASIS (Air-Sea Interaction Spar) buoy".
   f) Longbin Tao and Shunqing Cai "Heave motion suppression of a spar with a heave plate".

APPENDICES

Force and moment result on Surge, Heave and Pitch.

1. Force for surge analysis

	Total Force				
Frequency	492m	792m	1092m	1392	1692
0.035	100.864362	96.07936617	95.83690955	95.82435834	95.82370788
0.045	49008.1681	48866.68288	48865.6233	48865.61535	48865.61529
0.055	194749.418	194734.045	194734.0347	194734.0347	194734.0347
0.065	216528.8	216528.5474	216528.5474	216528.5474	216528.5474
0.075	163160.594	163160.5921	163160.5921	163160.5921	163160.5921
0.085	109113.136	109113.1356	109113.1356	109113.1356	109113.1356
0.095	71045.2609	71045.26089	71045.26089	71045.26089	71045.26089
0.105	46592.9891	46592.98905	46592.98905	46592.98905	46592.98905
0.115	31158.027	31158.02703	31158.02703	31158.02703	31158.02703
0.125	21326.0914	21326.09136	21326.09136	21326.09136	21326.09136
0.135	14943.8048	14943.80484	14943.80484	14943.80484	14943.80484
0.145	10708.5519	10708.55191	10708.55191	10708.55191	10708.55191
0.155	7834.56542	7834.565425	7834.565425	7834.565425	7834.565425
0.165	5842.02136	5842.021362	5842.021362	5842.021362	5842.021362
0.175	4432.53976	4432.539757	4432.539757	4432.539757	4432.539757
0.185	3416.78118	3416.781185	3416.781185	3416.781185	3416.781185
0.195	2672.11636	2672.116361	2672.116361	2672.116361	2672.116361
0.205	2117.53144	2117.531444	2117.531444	2117.531444	2117.531444
0.215	1698.48809	1698.488093	1698.488093	1698.488093	1698.488093
0.225	1377.6161	1377.6161	1377.6161	1377.6161	1377.6161
0.235	1128.88253	1128.882525	1128.882525	1128.882525	1128.882525
0.245	933.871011	933.8710107	933.8710107	933.8710107	933.8710107
0.255	779.365436	779.3654355	779.3654355	779.3654355	779.3654355
0.265	655.754238	655.7542381	655.7542381	655.7542381	655.7542381
0.275	555.959955	555.959955	555.959955	555.959955	555.959955

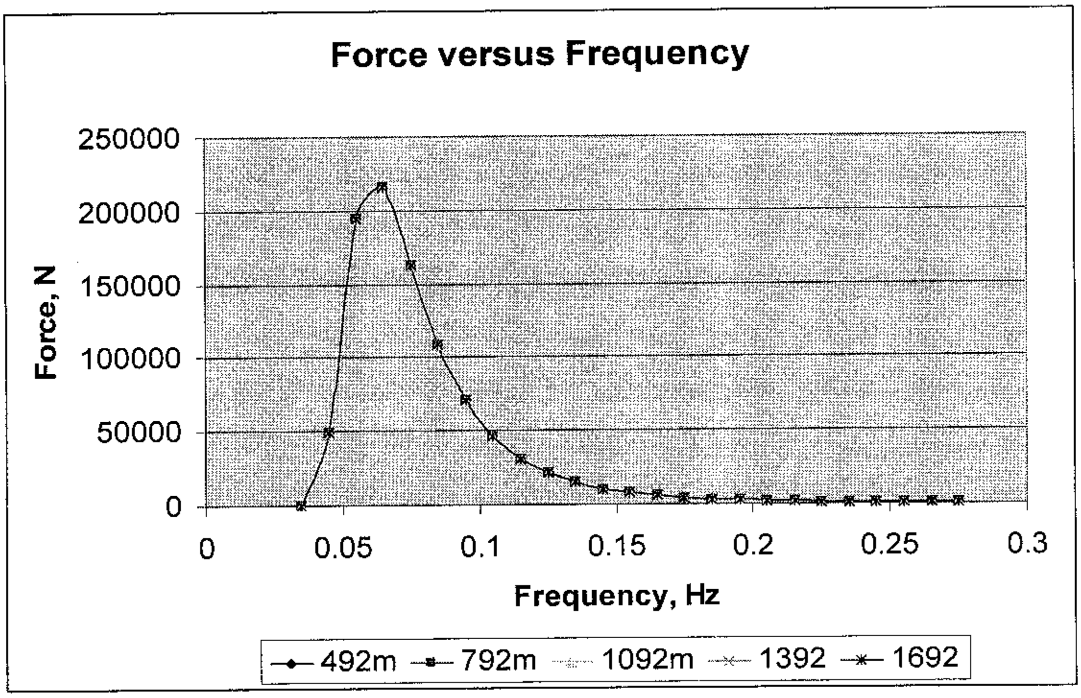

Graph A: Force versus Frequency for surge.

2. Force for heave analysis

	Total Force				
Frequency	492m	792m	1092m	1392m	1692m
0.035	178019.8961	170465.4783	170070.4262	170049.9187	170048.8545
0.045	1926026.78	1910937.462	1910824.022	1910823.17	1910823.163
0.055	1682995.052	1681699.53	1681698.661	1681698.66	1681698.66
0.065	673491.3225	673460.7901	673460.789	673460.789	673460.789
0.075	189170.6137	189170.3013	189170.3013	189170.3013	189170.3013
0.085	42491.03825	42491.03666	42491.03666	42491.03666	42491.03666
0.095	7979.216437	7979.216432	7979.216432	7979.216432	7979.216432
0.105	1.646861485	1.646861485	1.646861485	1.646861485	1.646861485
0.115	172.8973126	172.8973126	172.8973126	172.8973126	172.8973126
0.125	20.030989	20.030989	20.030989	20.030989	20.030989
0.135	1.973220192	1.973220192	1.973220192	1.973220192	1.973220192
0.145	0.164660891	0.164660891	0.164660891	0.164660891	0.164660891
0.155	0.011584414	0.011584414	0.011584414	0.011584414	0.011584414
0.165	0.000682991	0.000682991	0.000682991	0.000682991	0.000682991
0.175	3.34812E-05	3.34812E-05	3.34812E-05	3.34812E-05	3.34812E-05
0.185	1.34977E-06	1.34977E-06	1.34977E-06	1.34977E-06	1.34977E-06
0.195	4.39977E-08	4.39977E-08	4.39977E-08	4.39977E-08	4.39977E-08
0.205	1.12532E-09	1.12532E-09	1.12532E-09	1.12532E-09	1.12532E-09
0.215	2.11402E-11	2.11402E-11	2.11402E-11	2.11402E-11	2.11402E-11
0.225	2.33593E-13	2.33593E-13	2.33593E-13	2.33593E-13	2.33593E-13
0.235	-8.86265E-16	-8.86265E-16	-8.86265E-16	-8.86265E-16	-8.86265E-16
0.245	-1.06616E-16	-1.06616E-16	-1.06616E-16	-1.06616E-16	-1.06616E-16
0.255	-2.66644E-18	-2.66644E-18	-2.66644E-18	-2.66644E-18	-2.66644E-18
0.265	-4.18311E-20	-4.18311E-20	-4.18311E-20	-4.18311E-20	-4.18311E-20
0.275	-4.55985E-22	-4.55985E-22	-4.55985E-22	-4.55985E-22	-4.55985E-22

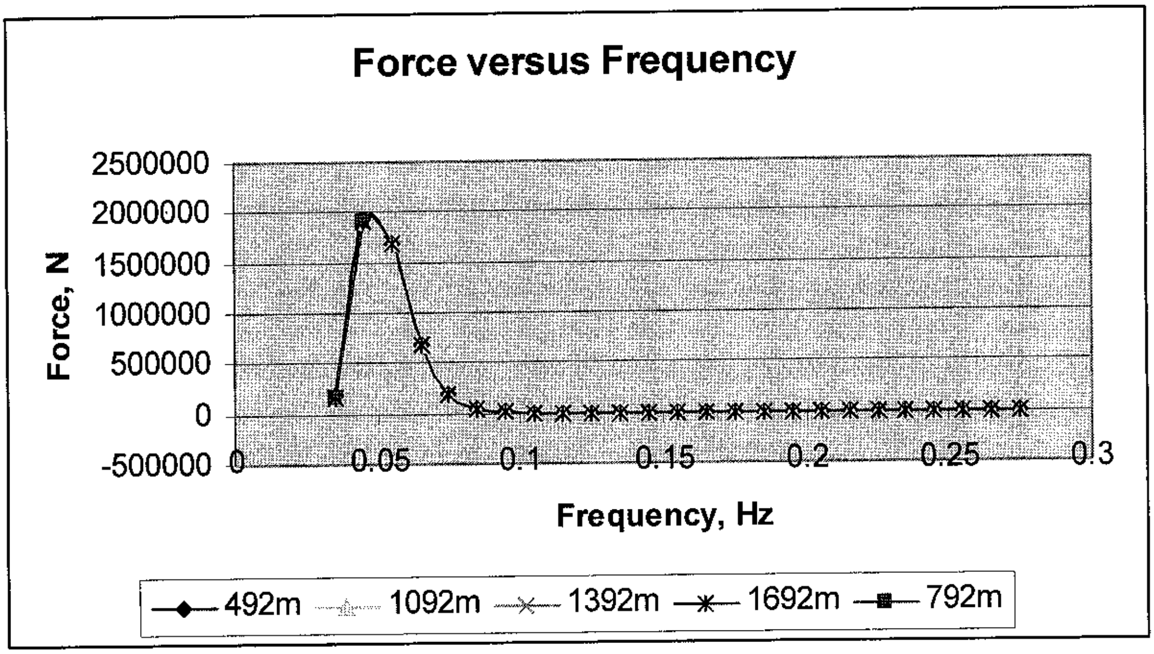

Graph B: Force versus frequency for Heave analysis

3. Moment for pitch analysis

	Total moment				
Frequency	492m	792m	1092m	1392m	1692m
0.035	-613.851857	-683.152165	-686.5799022	-686.7571187	-686.7663022
0.045	-1101892.85	-1103777.284	-1103791.341	-1103791.447	-1103791.448
0.055	-7057966.41	-7058197.251	-7058197.406	-7058197.406	-7058197.406
0.065	-10075702.4	-10075707.61	-10075707.61	-10075707.61	-10075707.61
0.075	-8757118.1	-8757118.172	-8757118.172	-8757118.172	-8757118.172
0.085	-6391066.52	-6391066.518	-6391066.518	-6391066.518	-6391066.518
0.095	-4406264.52	-4406264.521	-4406264.521	-4406264.521	-4406264.521
0.105	-3006432.39	-3006432.391	-3006432.391	-3006432.391	-3006432.391
0.115	-2068930.61	-2068930.611	-2068930.611	-2068930.611	-2068930.611
0.125	-1446821.51	-1446821.511	-1446821.511	-1446821.511	-1446821.511
0.135	-1030748.36	-1030748.357	-1030748.357	-1030748.357	-1030748.357
0.145	-748318.175	-748318.1747	-748318.1747	-748318.1747	-748318.1747
0.155	-553244.421	-553244.4209	-553244.4209	-553244.4209	-553244.4209
0.165	-416075.453	-416075.453	-416075.453	-416075.453	-416075.453
0.175	-317924.752	-317924.7524	-317924.7524	-317924.7524	-317924.7524
0.185	-246518.15	-246518.1502	-246518.1502	-246518.1502	-246518.1502
0.195	-193753.125	-193753.1255	-193753.1255	-193753.1255	-193753.1255
0.205	-154193.055	-154193.0554	-154193.0554	-154193.0554	-154193.0554
0.215	-124130.615	-124130.6154	-124130.6154	-124130.6154	-124130.6154
0.225	-100997.897	-100997.8973	-100997.8973	-100997.8973	-100997.8973
0.235	-82989.5266	-82989.52662	-82989.52662	-82989.52662	-82989.52662
0.245	-68818.2254	-68818.2254	-68818.2254	-68818.2254	-68818.2254
0.255	-57553.8787	-57553.87866	-57553.87866	-57553.87866	-57553.87866
0.265	-48516.0125	-48516.01246	-48516.01246	-48516.01246	-48516.01246
0.275	-41200.9355	-41200.93552	-41200.93552	-41200.93552	-41200.93552

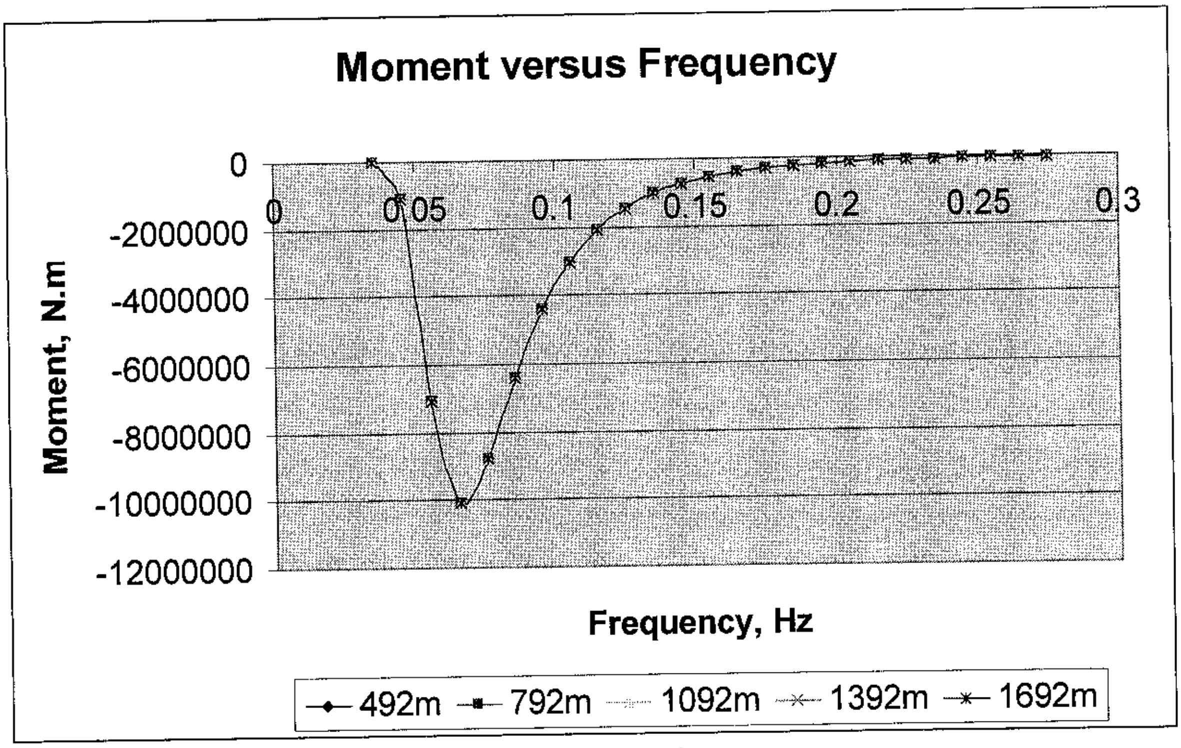

Graph C: Moment versus frequency for pitch analysis

-END OF REPORT-